IMAGE RESTORATION TECHNIQUES IN SPATIAL DOMAIN AND FREQUENCY DOMAINS

OSAMAH JASIM MADHLOOM

FACULTY OF ENGINEERING
UNIVERSITY OF MALAYA
KUALA LUMPUR

2017

IMAGE RESTORATION TECHNIQUES IN SPATIAL DOMAIN AND FREQUENCY DOMAINS

OSAMAH JASIM MADHLOOM

RESEARCH REPORT SUBMITTED TO FACULTY OF ENGINEERING, UNIVERSITY OF MALAYA, IN PARTIAL FULFILMENT OF THE REQUIREMENTS FOR THE DEGREE OF MASTER IN ENGINEERING

FACULTY OF ENGINEERING
UNIVERSITY OF MALAYA
KUALA LUMPUR

2017

UNIVERSITY OF MALAYA

ORIGINAL LITERARY WORK DECLARATION

Name of Candidate: Osamah Jasim Madhloom (I.C/Passport No:

Matric No: KGE 150014

Name of Degree: Master of Engineering (Telecommunication)

Title of Research Report ("this Work"): Image restoration techniques in spatial domain and frequency domains.

Field of Study: Image and signal processing

I do solemnly and sincerely declare that:

(1) I am the sole author/writer of this Work;
(2) This Work is original;
(3) Any use of any work in which copyright exists was done by way of fair dealing and for permitted purposes and any excerpt or extract from, or reference to or reproduction of any copyright work has been disclosed expressly and sufficiently and the title of the Work and its authorship have been acknowledged in this Work;
(4) I do not have any actual knowledge nor do I ought reasonably to know that the making of this work constitutes an infringement of any copyright work;
(5) I hereby assign all and every rights in the copyright to this Work to the University of Malaya ("UM"), who henceforth shall be owner of the copyright in this Work and that any reproduction or use in any form or by any means whatsoever is prohibited without the written consent of UM having been first had and obtained;
(6) I am fully aware that if in the course of making this Work I have infringed any copyright whether intentionally or otherwise, I may be subject to legal action or any other action as may be determined by UM.

Candidate's Signature Date:

Subscribed and solemnly declared before,

Witness's Signature Date:

Name:

Designation

ABSTRACT

A digital image is a numeric representation of a two-dimensional image. A recorded image is often contaminated with noise. Hence, image restoration is a fundamental research topic in the realm of image to obtain an optimal estimate of the original image given the degraded image.

In this study, Direct Inverse Filter, Wiener filter, and Complex Wavelet filter techniques are applied to eliminate the noise, thereby improving the quality of the restored image. They are analyzed, derived, and implemented using MATLAB software for reconstructing the degraded image. Two types of noise, Gaussian noise and Salt & Pepper noise with different levels of noise are used to contaminate the original image. Then, image quality metrics, namely; mean square error (MSE), peak signal-to-noise ratio (PSNR), and structural similarity index (SSIM) are applied to measure the quality of the restored images using the aforementioned image restoration techniques. Experimental and simulation results show that Constrained Complex wavelet filter is the best-performing image restoration technique followed by Wiener filler, and finally Direct Inverse filter.

ABSTRAK

Imej digital adalah perwakilan berangka bagi imej dua dimensi. Kebiasaanya, imej yang telah direkodkan akan mengandungi gangguan isyarat. Oleh itu, pemulihan imej merupakan topik penyelidikan asas dalam bidang imej untuk memperoleh anggaran optimum kepada imej asal yang telah diberikan oleh imej yang berkualiti rendah.

Dalam kajian ini, teknik penapisan songsang terus, penapisan Wiener, dan penapisan kompleks Wavelet digunakan untuk menghilangkan gangguan isyarat dan seterusnya meningkatkan kualiti imej yang dipulihkan. Imej tersebut akan dianalisis, diperoleh dan dilaksanakan mengguna perisian MATLAB untuk membina semula imej yang lebih baik. Terdapat dua jenis gangguan isyarat iaitu; gangguan isyarat Gaussian dan gangguan isyarat Salt & Pepper dengan tahap gangguan isyarat yang berbeza digunakan keatas imej asal. Seterusnya, metrik kualiti imej; iaitu purata ralat persegi, nisbah isyarat-ke-gangguan, dan indeks persamaan struktur digunakan untuk mengukur kualiti imej yang dipulihkan mengguna teknik pemulihan imej yang disebutkan diatas. Hasil eksperimen dan simulasi menunjukkan bahawa penapisan kompleks Wavelet adalah teknik pemulihan imej yang paling baik diikuti dengan teknik penapisan Wiener dan teknik penapisan songsang terus.

ACKNOWLEDGEMENTS

"In the name of Allah, the most beneficent and the most merciful"

First and foremost, I would like to thank Allah Almighty subhanahu wa-ta'ala for His endless blessing and giving me the perseverance to achieve what I have achieved today.

I would like to thank and appreciate my supervisor Professor Dr. Raveendran A/I paramesran for his continuous support, academically and personally, and great patience throughout the period it took to complete this thesis.

Above all, I would like to tip my hat to my family who have given me their unequivocal support for which my mere expression of thanks does not suffice. Specifically, I am heartfully thankful to my beloved parents, Jasim Madhloom and Muna Jabur, for their unconditional love, encouragements, guidance and support. I offer my regards and blessings to my siblings for their unconditional support in all aspects during my life. Furthermore, I would like to offer my sweet love and thanks to all my uncles and aunts.

My special thanks to my friends Haidar, Mustafa, Ethar, Khalil, Mohamad, Dhulfiqar, Ameer, for their guidance, help and support.

TABLE OF CONTENTS

LIST OF FIGURES

LIST OF TABLES

LIST OF SYMBOLS AND ABBREVIATIONS

CCD	:	Charge-Coupled Device
CSF	:	Contrast Sensitivity Function
DT-CWT	:	Dual Tree Complex Wavelet Transform
FR	:	Full Reference
ISNR	:	Improved Signal to Noise Ratio
IQA	:	Image Quality Assessment
MSE	:	Mean Square Error
PDF	:	Probability Density Function
PSNR	:	Peak Signal to Noise Ratio
RGB	:	Reed Green Blue
SNR	:	Signal to Noise Ratio
SSIM	:	Structural Similarity Index
WSNR	:	Weighted Signal to Noise Ratio

CHAPTER 1: INTRODUCTION

1.1 Research Background

Visual components of digital images are in principle a matrix of numerical values. Image processing operations use algorithms to manipulate these numerical values mathematically. Since these algorithms operate in predefined ways, it is possible to predict their behavior. By studying the underlying processes of enhancement algorithms, it is therefore possible to predict how they react in relation to different image properties and thereby establish an ideal order for their application. (Ledesma, S. A, 2015). A proposed framework for forensic image enhancement.

The recorded images are invariably contaminated with noise that arises from a number of sources and can be either multiplicative noise or additive noise. The principal sources of noise in digital images are:

I. If the image is scanned from a photograph made on film, the film grain is the source of noise. Noise can also be the result of the damage to the film, or be introduced by the scanner itself.
II. The imaging senor may be affected by environmental conditions during image acquisition.
III. If the image is acquired directly in a digital format, the mechanism for gathering the data can introduce noise.
IV. Insufficient light levels and senor temperature may introduce the noise in the image.
V. Electronic transmission of image data can introduce noise.
VI. Interference in the transmission channel may also corrupt the image.
VII. If dust particles are present on the scanner screen, they can also introduce noise in the image (Kaur, 2015a).

Thus, the image degradation can be modelled as shown in Figure 1.1 and mathematically formulated as follows:

$$g(x,y) = f(x,y) * h(x,y) + n(x,y)$$

where $g(x,y)$ is the degraded image, $f(x,y)$ is the original image, $h(x,y)$ is the degradation function, $n(x,y)$is the additive noise, and * indicates convolution.

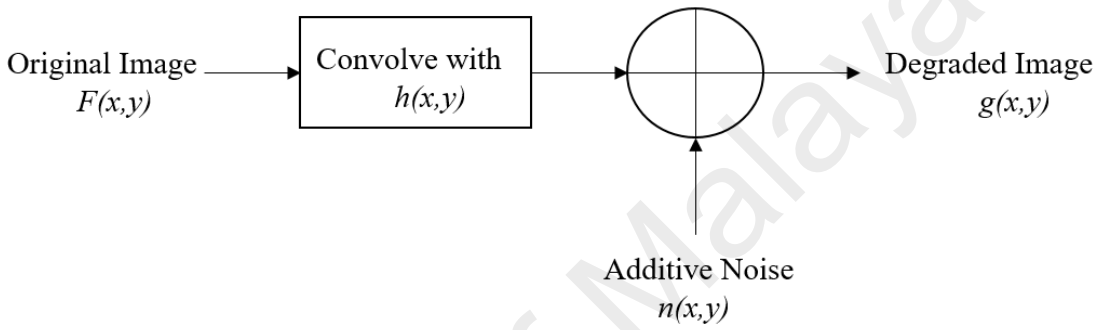

Figure 1.1 Image Degradation Model in Spatial Domain

1.2 Image Degradation Model in Spatial Domain

Due to the fact convolution in the spatial domain is the same as multiplication in the frequency domain, the equivalent representation of the image degradation model in the frequency domain is illustrated in Figure 1.1 and mathematically formulated as follows:

$$G(u,v) = H(u,v)F(u,v)N(u,v)$$

where (u,v) represents the spatial domain coordinates whereas the terms in capital letters as the Fourier transforms of the corresponding terms in the spatial domain

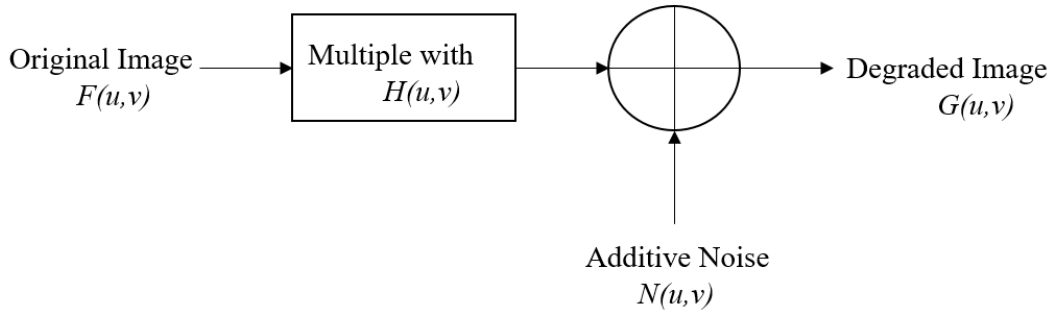

Figure 1.2 Image Degradation Model in Frequency Domain

1.3 Image Degradation Model in frequency Domain

In image processing, noise reduction and restoration of image is expected to improve the qualitative inspection of an image and the performance criteria of quantitative image analysis techniques Digital image is inclined to a variety of noise which affects the quality of image. The de-noising the image is main purpose in restoring the detail of original image as much as possible. The criteria of the noise removal problem depend on the noise type by which the image is corrupting. In the field of reducing the image noise several types of linear and nonlinear filtering techniques have been proposed. Different approaches for reduction of noise and image enhancement have been considered, each of which has their own limitation and advantages (Rani, 2013).

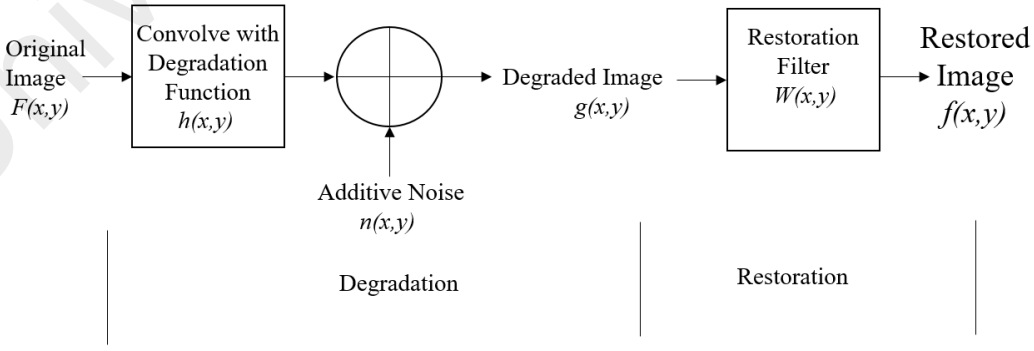

Figure 1.3 Image Degradation and Restoration Model in Spatial Domain.

The objective of image restoration is clear-cut which is to obtain an optimal estimate $\hat{f}(x, y)$ of the original image $f(x, y)$ given the degraded image(x, y), some information in regard to statistical properties of the additive noise.

1.4 Problem Statement

The recorded image may have degraded due to contaminated with different variances of Gaussian noise and different densities of salt and pepper noise.

1.5 Objectives of Research

The main objective of this research project is to derive image restoration techniques and implement the derived image restoration techniques in MATLAB to restore a degraded image. The following outlines the detailed objectives of this research project:

I. To restore a degraded image using Direct Inverse Filter.
II. To restore a degraded image using the Wiener Filter.
III. To restore a degraded image using discrete wavelet transform.
IV. Comparison between Direct Inverse Filter, Wiener Filter and Wavelet Transform Filter.

1.6 Research Report Organization

Chapter 2 discusses the related works comprehensively. Chapter 3 outlines the research implementation as well as the image degradation model which comprises of noise models. Additionally, this chapter also discusses the image quality assessments techniques, as well as this chapter presents the detailed derivations of each image restoration techniques employed to reconstruct the different types of noise. Chapter 4 presents the restored images, computes and tabulates the image quality metrics, discuss features, challenging, as well as drawbacks of the image restoration techniques, and

compares the image restoration techniques. Chapter 5 summarizes the research with direction for future development.

CHAPTER 2: LITERATURE REVIEW

2.1 Restoration of digital images

Image restoration is the operation that corrects degraded images and reconstructs a good quality signal from an image of mediocre quality. The restoration of the photograph could be done using varieties of editing techniques for the purpose of removing aging effects and visible damage.

2.2 Image degradation model

Let $X = \{x_{ij}\}$ be a two-dimensional random field defined on the grid $L = \{(ji), 0 \leq i < M\ 0, \leq j < N\}$, representing a true but unobservable image x_{ij} measures the intensity of the color, the gray level of the pixel at position (i, j). The available data is y, a measurable version of x but affected by degradations due to noise and/or blurring which try to recover an image from its fuzzy or noisy version. In image restoration, the linear model of observation is expressed by:

$$Y = H_{ij} + n$$

In this formulation, n represents an additive perturbation often considered as centered Gaussian white noise, while H represents the matrix of the system spread function. Sometimes, degradation involves nonlinear transformation and multiplicative noise. This usually happened in the presence of speckle in radar images or grains on X-ray films. The problem of recovering x is much more difficult. The matrix H and the statistical characteristics of the noise n are assumed to be known. Nevertheless, this assumption is not always met and these quantities must also be estimated. Restoration techniques, therefore, require the modeling of the degradation and the image itself and then apply an inverse procedure to obtain an estimate of the true image (Pillai & Khadagade, 2017).

In mathematical terms, image restoration is an inverse problem badly posed. A problem is well posed if its solution exists, therefore it's unique and depends continuously on the observed data. These are the so-called conditions of Hadamard for a problem of being well laid. In image restoration, the single solution does not exist. Moreover, it is impossible to obtain the true solution from erroneous or noisy data. The regularization of the problem by incorporating the information a priori in addition to the information provided by the observation makes it possible to define an admissible class of solutions.

2.3 Measuring the Quality of Restoration

2.3.1 Standards for Measuring Restoration Quality

In image restoration, the most commonly used quantitative measurements are improved signal-to-noise ratio (ISNR), Mean Squared Error (MSE) and the peak of the signal-to-noise ratio, PSNR (Peak Signal-to-Noise Ratio) respectively. These are defined as follows:

$$ISNR = 10.\log_{10}\frac{\sum_{i,j}[x(i,j) - y(i,j)]^2}{\sum_{i,j}[x(i,j) - \hat{x}(i,j)]^2}$$

$$MSE = \frac{1}{M.N}[\sum_{i,j}[x(i,j) - \hat{x}(i,j)]^2$$

$$ISNR = 10.\log_{10}\left[\frac{MAX_p^2}{MSE}\right]$$

Where x, y, and x represent the original (true) image, the degraded image, and the restored image respectively. MAX_p, is the maximum intensity of the gray levels. Obviously, these measurements are used exclusively for simulation cases where the original image is available. As a result, they do not always reflect the perceptual properties of the human visual system. However, they provide an objective standard by

which different restoration techniques are compared. When image restoration quality is measured with two different measurements, three important aspects are considered in a comparative evaluation of the two measurements. These important characteristics are; accuracy, precision, and direction of measurement.

2.3.2 Accuracy of the Quality Measurement of Restoration

A precise measurement of the restoration quality of an image must closely reflect the subjective appreciation of the human observer. However, there is no clear definition of image quality and its exact measurement procedure. Therefore, there is no reliable criterion for assessing the accuracy of a measure of restoration quality. Precision is the expression of a small relative variability in the measurement process. Let us assume set of similar images distorted by the same type of blur and with the same amount of noise. These images have been restored by the same restore operator. A high-precision measurement of image restoration quality, when applied to these restored images, should produce a set of small-scale propagation measurements. The smaller the spread, the more accurate the measurement.

2.3.3 Meaning of the Quality of Restoration

The improvement on the SNR is defined as the difference between the signal to noise ratio of the images before and after restoration. A positive SNR improvement indicates that the quality of the distorted image is improved, while the negative SNR indicates deterioration of the image. The zero value of the SNR improvement indicates no improvement or deterioration.

2.4 Image restoration

Numerous methods have been proposed to solve and regularize the equation of the linear model of observation. However, considering direct restoration approaches, either

a stochastic model or a deterministic model for the original image can be used. In both cases, the model represents a priori information about the solution that can be used to make the problem well posed. Stochastic regularization is based on statistical considerations of images and noise as stochastic or random processes. If the only random process in question is the additive noise n, then the solution of the minimum estimate of the quadratic mean of x will be called a regression problem.

$$\min E\{\|x - \hat{x}\|\}$$

However, if the image x is also considered as a random process, with the knowledge of $R_{xx} = E\{xx^T\}$ which is the covariance matrix of x, and $R_{nn} = E\{nn^T\}$ which is the noise covariance matrix, then the problem will be subject to a Wiener estimate. In this case, the linear estimate which minimizes the equation of the quadratic mean of x is given by:

$$\hat{x} = R_{xx}\boldsymbol{H}^T(\boldsymbol{H}\, R_{xx}\boldsymbol{H}^T + R_{nn})^{-1}\mathrm{y}$$

This equation can be rewritten and solved in the domain of the discrete frequencies which leads to Fourier implementation of the Wiener filter. There are several methods that can be used to estimate the statistical parameters needed to run the Wiener filter. They can be estimated by parametric and nonparametric approaches. Examples of techniques that fall within this framework can be found in (Pillai & Khadagade, 2017) (Li, Meunier, & Soucy, 2006).

2.4.1 Image restoration by Wiener filter

The Wiener filter is a spatially invariant linear filter in which the impulse response is chosen so that it minimizes the mean square error between the ideal image and the

restored image. This minimization of the mean squared error between the original image and the restored image is written as follows:

$$EQM = E[(o(x,y) - \hat{o}(x,y))^2]$$

where o is the ideal image, ô is the restored image and E is the mathematical expectation. This criterion tends to reduce the difference between the restored image and the ideal image. The solution to this minimization problem is easily defined in the spectral domain as the Wiener filter (Bovik, 2010).

$$\hat{o}(u,v) = I(u,v)\frac{H^*(u,v)}{H^*(u,v)H(u,v) + \frac{S_B^2(u,v)}{S_O^2(u,v)}}$$

Where H and H* are the frequency equivalent of the impulse response and its complex conjugate, respectively. While S_O and S_B are the spectral powers of the ideal image and the noise, respectively.

In a typical situation where an image is noisy, this approach makes a compromise between reverse filter restoration and noise suppression for frequencies where the frequency response is close or equal to zero (Bovik, 2010). Although it is easy to implement, this approach requires a comprehensive knowledge of the noise spectrum. The least squares method with constraints is an alternative to overcome the problem of the inverse filter. This approach is implemented using predetermined prior information about the original image as a regularization parameter (Bovik, 2010). Also, the method is based on the minimization of the quadratic difference between the acquired image (ô) and the estimated image (o).

2.4.2 Image Recovery by Reverse Filter

The inverse filter is undoubtedly one of the first approaches to be used in the deconvolution of images since 1960. The inverse filter is generally a linear filter whose impulse response is the inverse of the degradation function suffered by the image. The implementation of this filter in the space domain can be difficult. But on the contrary, the spectral equivalent is generally easier. In the absence of any noise, the equation can be written as follow:

$$I(u,v) = (u,v)O(u,v) => \hat{O}(u,v) = \frac{I(u,v)}{H(u,v)}$$

Where ô is the restored image close to the real image *o*.

The advantage of this technique, it requires only the knowledge of the impulse response. It is very fast in terms of computing time and allows the perfect restoration of the image. In a situation where noise is presented in the image, its effects are irremediably amplified by this technique. This is also the case for frequencies close to the cutoff frequency. Therefore, this method is not desirable when noise is presented. To remedy the shortcomings of this approach and overcome its sensitivity to noise, several restoration filters have been developed which collectively are called "square least-squares filters".

2.4.3 Image Recovery by Wavelets

Wavelets are functions of L^2 (R). These functions are generated by a translation of the localization parameter u ∈ R and *a* dilation of the scaling factor s ∈ R from a single function called wavelet-mother ψ ∈ L^2 (R), of zero average and which Oscillates locally.

Wavelets originate in the theory of signal processing, whereas it is necessary to find means and tools to approximate functions. Their roots are generated by functional analysis, mainly from advanced concepts on vector spaces and their properties. Jean Morlet and Alex Grossman were the two geophysicists that invented wavelets in the early 1980s. Gabor subsequently decomposed a signal in frequencies over several intervals. This help to reduce the problem of representation of the signal, particularly, by comparing the intervals with the several pieces of oscillating curves of different frequencies. These pieces of curves are indeed small waves, commonly called wavelets, whose size are variable. The wavelet transforms are found in both the continuous and the discrete domain. They work on all possible shifts or compressions of the signal under consideration. The notions of multi-resolution analysis by Mallat's work (Mallat, 1989) have introduced powerful new tools, linking orthogonal wavelets to mirror filters. By this method, it is now possible to approximate a signal φ by two main elements: A scaling function ψ obtained by a low-pass filter, and δ by a high-pass filter. The low-pass filter will give us the signal summary macroscopically, and the details of the said signal are obtained at the output of the high-pass filter. It should be remembered that filters are mathematically well-defined elements and therefore have established properties. The filter bank approach has therefore been used extensively in telephony. However, the literature refers it to several types of wavelets, characterized by their respective bases.

2.4.4 Discrete wavelets

In the case where the parameters (s, u) are discretized, the wavelet ψ (t) is constructed from a so-called scale function. The basic principles of the multiresolution analysis were laid down by Mallat (Mallat, 1989). A multi-resolution analysis of L^2 (R) makes it possible to organize the information contained in a 1D signal into a set of approximation

and detail signals at successive levels of resolution j = 1, ..., J. The detail signal at a stage j> 1 is by definition equal to the difference between the approximation of the original signal at stage j - 1 and its approximation at stage j. Thus, from the coarsest scales to the finest scales, more and more precise representations of the initial signal accede.

2.4.5 Wavelets with compact supports

Note that to simplify the implementation of the wavelet transform, finite impulse response filters are chosen for analysis and synthesis. This amounts to imposing a ψ (t) to be bonded and compactly supported. Wavelets of this type have been studied by (Daubechies, 1988).

2.4.6 Biorthogonal wavelets

It appears that the orthonormal wavelets with compact support must satisfy some strict conditions. The non-linearity's of the phase of the analysis and synthesis filters is a disadvantage, especially in compression applications. To circumvent this problem, the orthogonality constraint is then released (Cohen, Daubechies, & Feauveau, 1992).

2.4.7 Multi-dimensional Extension

It is possible to extend the notion of wavelet decomposition to multidimensional signals, in particular to digital images. In the latter case, the decomposition of the original image I_0 (m, n), m, n $\in$ {1, ..., N} is recursively made separately. For each stage j = 0, ..., J - 1, the approximation image aj (m, n), m, n $\in$ {1, ..., N $/2^J$} is treated in 2 steps by successively analyzing it. This decomposition process results in a sub image approximation aJ (m, n), m, n $\in$ {1, ..., N $/2^J$} at the stage J and 3 sub pictures detail wj, o (m, N) at each stage j oriented horizontally (o = 1), vertically (o = 2) and diagonally (o = 3). Thus, the transformed two-dimensional discrete dyadic and separable wavelet has

the advantage of being a simple transformation to implement and not redundant (the total number of coefficients of approximation and wavelets at each stage j is equal to the number of pixels of the initial image). Note, however, that there are non-separable wavelet decompositions (Kovacvic & Sweldens, 2000).

2.4.8 Wavelet transformations M bands

A multi-resolution analysis in M bands of L^2 (R) (Steffen, Heller, Gopinath, & Burrus, 1993) uses a scaling function $\psi 0$ (t) $\in$ L^2 (R) and M -1, M $\geq$ 2 wavelets. The approximation signals are obtained by a succession of orthogonal projections of the original signal on a nested sequence of firm vector subspaces. This type of transformation has the advantage of finer representations in frequency. It also has the advantage of offering more freedom for the choice of filters. For example, it is possible to generate orthogonal compact support wavelets with symmetric filters, which is not the case for dyadic wavelets (Steffen et al., 1993).

2.4.9 Second generation wavelets

The second - generation wavelet transformations (Sweldens, 1996) is being preferred to the first - generation transformations described above. Indeed, its principle is more intuitive and it's based on the concept of the so-called facelift. There are three parts which is:

- At a set point j, the set of coefficients $a_j(n)$ is divided into coefficients with even and odd positions.
- The spatial redundancy present at the level of the approximation signal is exploited by predicting the coefficients at even positions from those in odd positions thanks to a prediction operator P.
- The approximation signal a_{j+1} (n) at the stage j + 1

This new decomposition structure calls for the following comments as follows:

- The intrinsic structure of this decomposition scheme guarantees its reversibility without any constraint on the operators U and P. This lack of constraint facilitates the design of these operators.
- Quantizers can be included in the operators P and U. In this case, if the original signal a_0 (n) is an integer, the approximation and wavelet coefficients are also integer values.

It can be observed that any bi-orthogonal wavelet decomposition associated with filters can be implemented by means of a finite number of lifting levels followed at the output of multiplications by two non - zero constants. The interest of representing the classical filter bank in the form of a facelift is that it is easy to verify different useful properties of wavelets. In practice, a very wide choice is presented for the operators P and U which can be linear or nonlinear. The 5/3 (Sweldens, 1996) transform is one of the most successful and used decompositions of the second generation.

2.4.10 Extensions of wavelet transformation

Despite its interesting properties, the transformed discrete dyadic and separable wavelet has several limitations. These limitations include lack of translation invariance and relative poverty in directional information. Thus, other multi resolution decompositions have been devised to remedy these problems. In the following, we present some of these decompositions most used in image processing.

2.4.11 Adjustable pyramids

Adjustable pyramids (Simoncelli & Farid, 1996) are multi-scale, multi-oriented transformations in which the image is decomposed into stages of O sub bands localized

to different orientations. This decomposition is done by the projection of the image at each stage $j \in \{1, ..., J\}$ on a chosen number O of oriented filters. These filters have the particularity of ensuring the property of the adjustability. Filters are oriented if they form copies of each other at different orientations. This property is ensured by the possibility of expressing each oriented filter localized to an orientation $o = 1, ..., O$ as a linear combination of a set of basic filters.

In addition, the decomposition into oriented pyramids is an invariant transformation by translation and rich in directional information. It also allows flexibility for the choice of the number of orientations O. All these reasons make orientable pyramids a powerful tool and widely used in image processing especially for classification (Beferull-Lozano, Xie, & Ortega, 2003). Nevertheless, the orientable pyramids have the disadvantage of being heavily redundant. Indeed, the number of coefficients at the output of the pyramid is equal to (40/3) times the number of initial coefficients.

2.4.12 The wavelets by the filter bank approach

A filter bank is an approach that is best known for the design of wavelets. A signal can be distributed on M bands, in this case, we speak of M-bands wavelet transform (Calderbank et al., 1998), (with $M \geq 2$). The filter banks are generally of two types which are analysis and synthesis.

a. The analysis filters, break down a signal input so that it is distributed on M bands.
b. Synthesis filters perform the inverse operation of the analysis filters. For M input signal bands, they are recomposed to produce a single output signal

2.4.13 Wavelets using the Lifting-scheme approach

The basic idea behind the facelift is that it provides a simple relationship between all multi resolution analyzes that share the same high pass filter or low pass filter. The wavelet can, therefore, be seen as a linear combination of scale functions, where the coefficients are given by the high-pass filter. The lifting scheme is a process of wavelet construction, better than the filter bank approach. One of its most important features is that they allow for any filter bank based on the facelift, to automatically satisfy the property of perfect reconstruction (Xiong, Tian, & Liu, 2007).

2.4.14 The complex wavelet transform in dual tree

To remedy the limitations of the 2D wavelet transform DWT, (Selesnick, Baraniuk, & Kingsbury, 2005) defined the complex 2D wavelet transform in a dual tree. Indeed, Kingsbury originally designed the complex 2D wavelet transform (Selesnick et al., 2005) to generate complex details of coefficients, this transformation is then 2 times redundant. The complex 2D wavelet transforms in a dual (2D DT-CWT) wavelet is implemented by two complex 2D wavelet transforms operating in parallel called primary and dual trees respectively.

The decomposition of an image I (m, n) by the primary and dual trees provides two sub-images approximations $a_1(m,n)$ and $a'_1(m,n)$ with complex coefficients. In addition, 3 sub-images of W 1, o (m, n), and $o \in \{1, 2, 3\}$ will be provided with diagonally and vertically oriented diagrams at the output of each tree. Thus, this decomposition allows a better directional selectivity than the DWT at the price of a redundancy factor equal to 4. It also has an additional advantage of being invariant by translation.

2.4.15 The transformed two-dimensional wavelet M bands into a dual tree

As shown in the previous transformations, a compromise between a minimum of redundancy and a wealth of directional information is a real challenge. It is in this context that the transformed 2D M-band dual-wave (2D DT-MWT) wavelet has been introduced by (Chaux, Duval, & Pesquet, 2006). This wavelet is aimed to combine the advantages of the M band transforms, namely the flexibility of choosing filters and the selectivity in frequency as well as the directionality and the invariance by translation ensured by the dual tree decomposition. A 2D DT-MWT is based on the decomposition of an original image I (p, q), p, q ∈ {1, ..., N} by two transformations M separable two-dimensional bands associated respectively with a primary tree and Dual shaft. The filter banks h_0,..., h_M and h'_0 ,...,h'_M associated with the primary tree and the dual tree form pairs of Hilbert. The decomposition of the image I (p, q) by the primary and dual trees results in two approximate images $a_1(p,q)$ and $a'_1(p,q)$ as well as M-1 sub bands detail $w_{1,m,m'}$((m, m') m,m′ ∈ {1,...,M −1}, (m,m′) ≠(0, 0) to the output of each tree. To obtain directional sub bands, a linear combination of the signals $w_{1,m,m'}(p,q)$ and $w'_{1,m,m'}(p,q)$ is performed.

The 2D DT-CWT characterizes only 6 different directions and it has the advantage of giving the user the free choice of the number of directions by adjusting the parameter M. This is done independently of the redundancy factor that remains always equal to two (2). It is noted that the 2D DT-MWT achieves a better compromise between directional selectivity and redundancy factor. The latter also has the advantage of being invariant by translation. Finally, it has the advantage of offering more freedom for the choice of filters compared to the 2D DT-CWT as the use of orthogonal compact support wavelets with symmetric filters. In this respect, it has been successfully used in image

processing (Chaux et al., 2006) and it would be of considerable interest to characterize images in the context of image search.

2.4.16 Application of decomposition M-bands in dual tree to denoising

The multidimensional decomposition of the complex dual-complex transform has already been shown to be effective in other denoising work. Specifically, it's very effective in video processing (Selesnick & Li, 2003) or satellite imagery(Jalobeanu, Blanc-Féraud, & Zerubia, 2003). In this section, it will be shown that the M-band transform in a dual tree also achieves very good performances in image denoising. Furthermore, it performs better than the method which is based on M-band wavelet transforms and even often the decomposition into a dual dyadic tree. The images of particular interest are usually the ones containing a lot of oriented and textured information like seismic images. Different families of wavelets have been tested, the results obtained were corresponded with those obtained by Meyer wavelets [Tennant, Rao, 2003]. This is because, the wavelets are declined in M-bands for whatever M. Curvelets have demonstrated their effectiveness in denoising (Starck, Candès, & Donoho, 2002) as well as decompositions in dual M-bands (Chaux et al., 2006). Although the formalisms that led to these two methods are totally different, the fact remains that these two transformations provide directional analyzes.

2.4.17 Quaternionic wavelets

Although the complex 2D dual-tree algorithm is associated with wavelet functions with many qualities such as directionality and quasi-invariance by translation. But one can wonder about the answer given by this construction in relation to the problem originally laid down, namely the construction of a 2-D analytic wavelet function. Particularly, this point was not discussed in the founding articles concerning complex 2-D wavelets. We have conducted a reflection on this point from Bülow's work and the definition of a

really analytic 2-D wavelet appeared only very recently in the papers of Chan et al.(Chan, Choi, & Baraniuk, 2008).

The presence of two complex numbers to define the analytic signal leads to a certain ambiguity in the definitions of the deduced information. Indeed, because of the structure, two norms and two angles was calculated which is difficult to explain their link or propose a strategy of fusion. Therefore, logically in the later work of Bülow on the quaternionic analytic signal has been recently proposed a quaternionic analytic wavelet decomposition by (Chan et al., 2008).

CHAPTER 3: RESEARCH METHODOLOGY

3.1 Flow Chart of Image Degradation/Restoration

The original image is degraded by either Gaussian Noise or Salt and Pepper noise. Various levels of noise are added to the image. Then, image restoration methods such as Direct Inverse Filter, Wiener Filter, and Complex Wavelet Filter. The flowchart of the image degradation and restoration is shown in Figure 3.1.

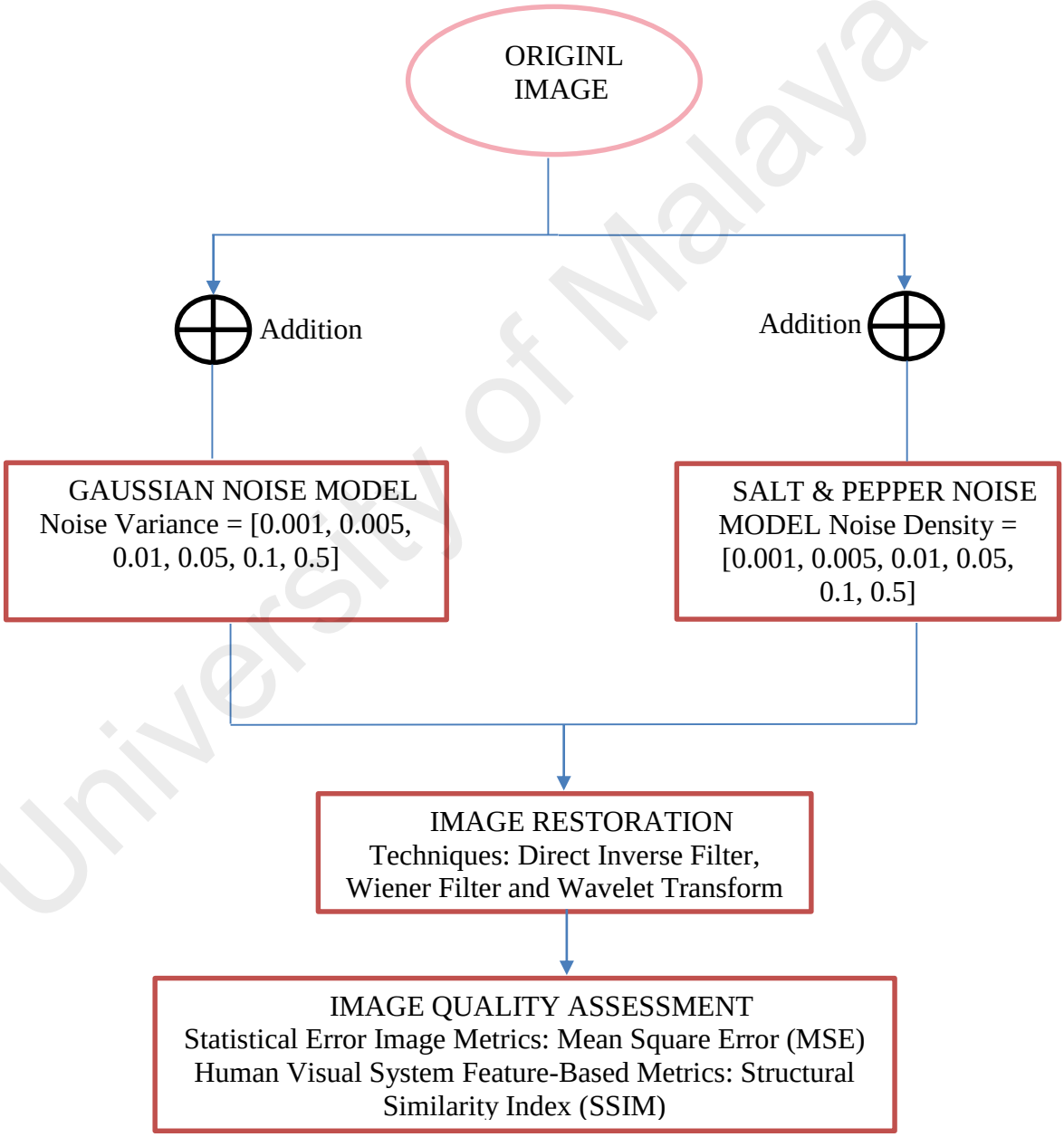

Figure 3.1 Flow chart of Image Degradation/ Restoration

3.2 Noise model

Noise is an unwanted information present in an image. Such unwanted information in an image can be removed with filters. In digital image processing, filters can be applied on an image in two ways, which include spatial and frequency domain. This paper mainly deals with the application of spatial domain filters on noisy images for the purpose of identifying the efficiency of the filters in terms of enhancing the quality of the image by removing the noise present on it (Swaminathan, 2016). Generally, an image gets affected by noise during its acquisition, transmission and storage. There are several ways that noise can be introduced into an image, depending on how the image is created. For example, If the image is scanned from a photograph made on film, the film grain is a source of noise. Noise can also be the result of damage to the film, or be introduced by the scanner itself. If the image is acquired directly in a digital format, the mechanism for gathering the data (such as a CCD detector) can introduce noise. Electronic transmission of image data can introduce noise(Kaur, 2015b).

There are two common types of noise models in image processing, namely Gaussian noise model and salt and pepper noise model.

3.2.1 Gaussian noise model

The random noise that enters the system can be modelled as Gaussian or normal distribution. The Gaussian distribution is a well-known bell-shaped curve. This is mathematically denoted as F = S ± Na, where Na is the Gaussian probability density function (PDF) and S is the noiseless image. The Gaussian noise affects both the dark and light areas of an image. The probability density function of Gaussian noise is mathematically expressed as follows: The Gaussian distribution is

$$P(z) = \frac{1}{\sigma\sqrt{2\pi}} e^{-\frac{(z-m)^2}{2\sigma^2}}$$

whereas the mean and variance of Gaussian noise are as follows:

mean, m=a

variance, $\sigma^2 = b^2$

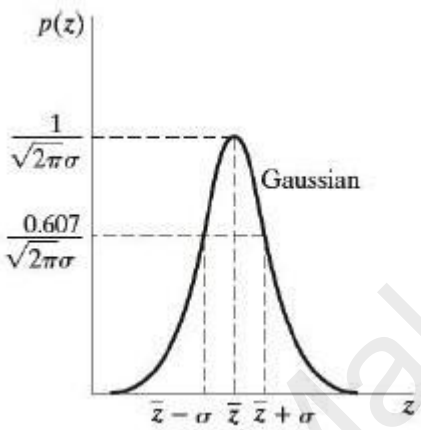

Figure 3.2 probability Density Function (Swaminathan, 2016).

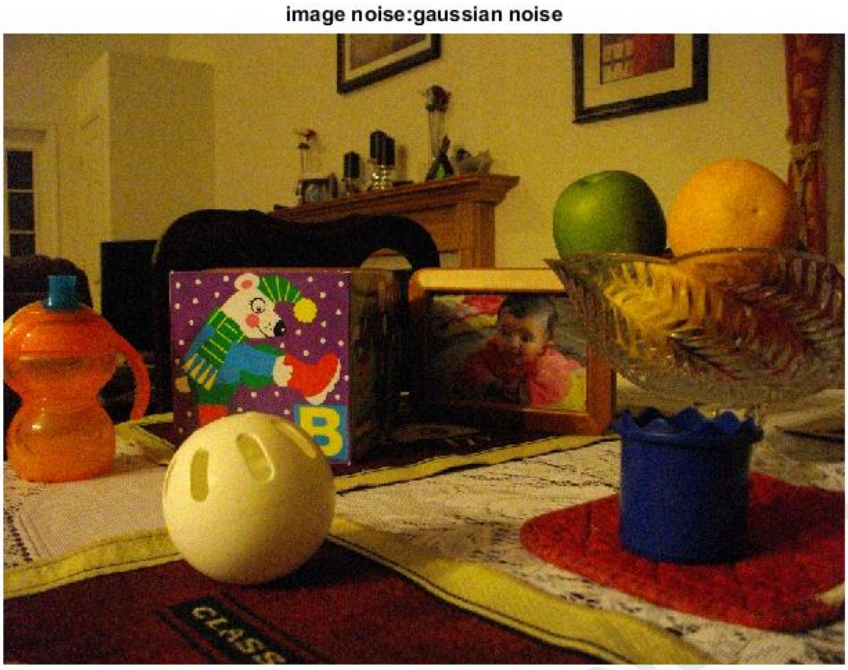

Figure 3.3 Gaussian Noise (Mean=0; Variance=0.001).

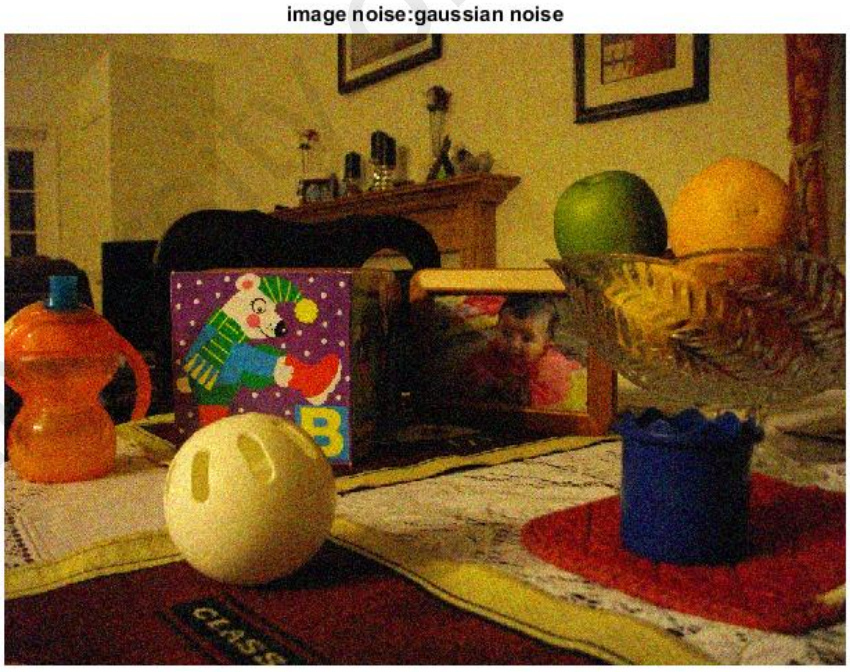

Figure 3.4 Gaussian Noise (Mean=0; Variance=0.005).

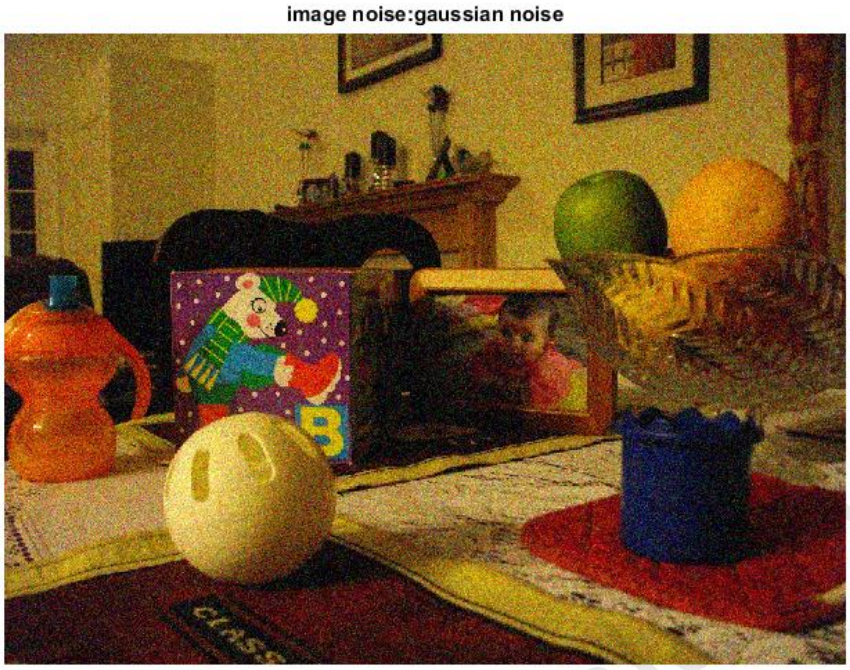

Figure 3.5 Gaussian Noise (Mean=0; Variance=0.005)

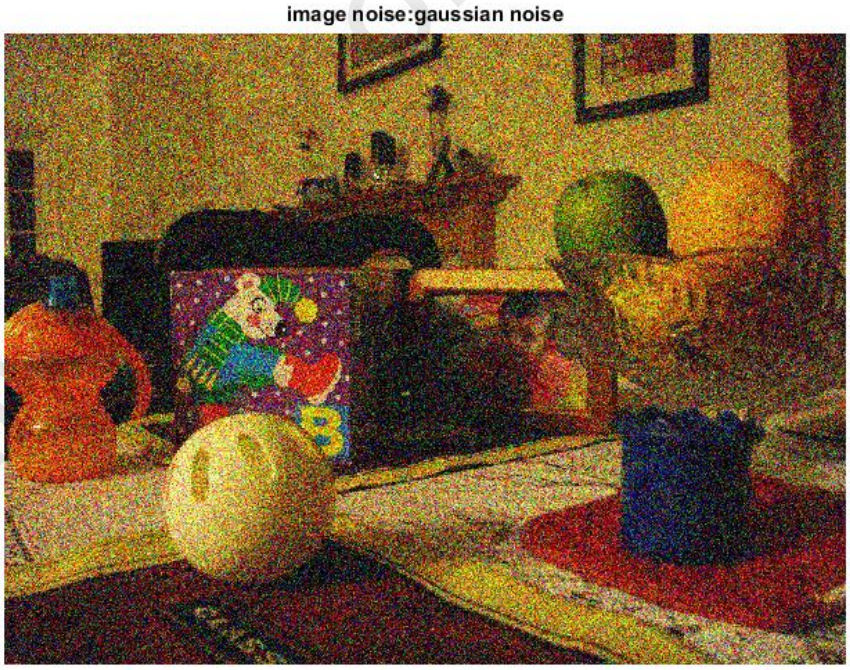

Figure 3.6 Gaussian Noise (Mean=0; Variance=0.05)

Figure 3.7 Gaussian Noise (Mean=0; Variance=0.1)

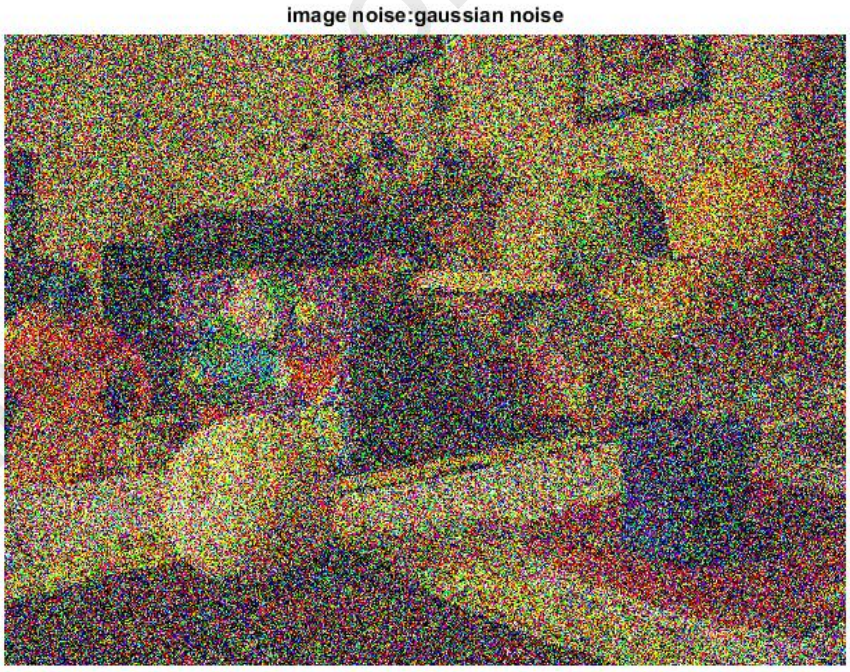

Figure 3.8 Gaussian Noise (Mean=0; Variance=0.5)

3.2.2 Salt and pepper noise model

For this kind of noise, conventional low pass filtering, e.g. mean filtering or Gaussian smoothing is relatively unsuccessful because the corrupted pixel value can vary significantly from the original and therefore the mean can be significantly different from the true value. A median filter removes drop-out noise more efficiently and at the same time preserves the edges and small details in the image better. Conservative smoothing can be used to obtain a result which preserves a great deal of high frequency detail, but is only effective at reducing low levels of noise. In salt and pepper noise (sparse light and dark disturbances), pixels in the image are very different in color or intensity from their surrounding pixels; the defining characteristic is that the value of a noisy pixel bears no relation to the color of surrounding pixels. Generally, this type of noise will only affect a small number of image pixels. When viewed, the image contains dark and white dots, hence the term salt and pepper noise. Typical sources include flecks of dust inside the camera and overheated or faulty CCD elements.

Salt and pepper noise is an impulse type of noise, which is also referred to as intensity spikes. This is caused generally due to errors in data transmission. It has only two possible values, a and b. The probability of each is typically less than 0.1. The corrupted pixels are set alternatively to the minimum or to the maximum value, giving the image a “salt and pepper” like appearance. Unaffected pixels remain unchanged. For an 8-bit image, the typical value for pepper noise is 0 and for salt noise 255. The salt and pepper noise is generally caused by malfunctioning of pixel elements in the camera sensors, faulty memory locations, or timing errors in the digitization process.(Garg & Kumar, 2012).

Salt and pepper noise is sometimes called impulse noise or spike noise or random noise or independent noise. In salt and pepper noise (sparse light and dark disturbances),

pixels in the image are very different in color or intensity unlike their surrounding pixels. Salt and pepper degradation can be caused by sharp and sudden disturbance in the image signal. Generally, this type of noise will only affect a small number of image pixels. When viewed, the image contains dark and white dots, hence the term salt and pepper noise. Typical sources include flecks of dust inside the camera and overheated or faulty (Charge-coupled device) CCD elements. An image containing salt-and-pepper noise will have dark pixels in bright regions and vice versa. This type of noise can be caused by dead pixels, analogue-to- digital converter errors and bit errors in transmission.(Garg & Kumar, 2012) the probability density function of salt and pepper noise is as follows:

$$P(Z) = \begin{cases} p_{a \text{ for } z=a} \\ p_b \text{ for } z = b \\ 0 \text{ otherwise} \end{cases}$$

the mean and variance of salt pepper noise are as follows:

mean, $m = aP_a + bP_b$

$$\sigma^2 = (a - m)^2 P_b + (b - m)^2 P_b$$

and the cumulative density function of salt and pepper noise is:

$$\begin{cases} 0 \text{ for } z < a \\ p_a \quad \text{for } a \leq z < b \\ p_a + p_b \quad \text{for } b \leq z \end{cases}$$

Figure 3.9 Salt and Pepper Noise (Density=0.001)

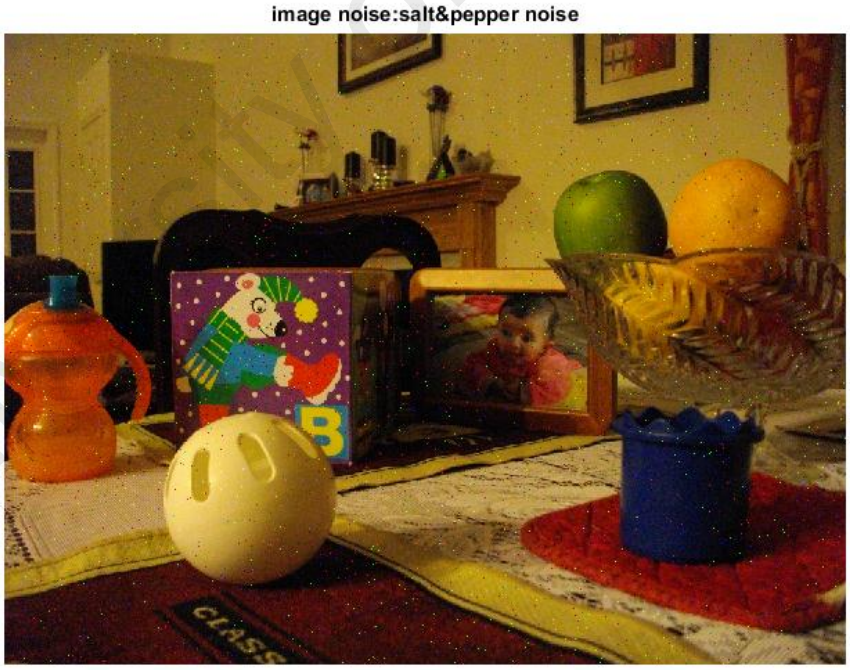

Figure 3.10 Salt and Pepper Noise (Density=0.005)

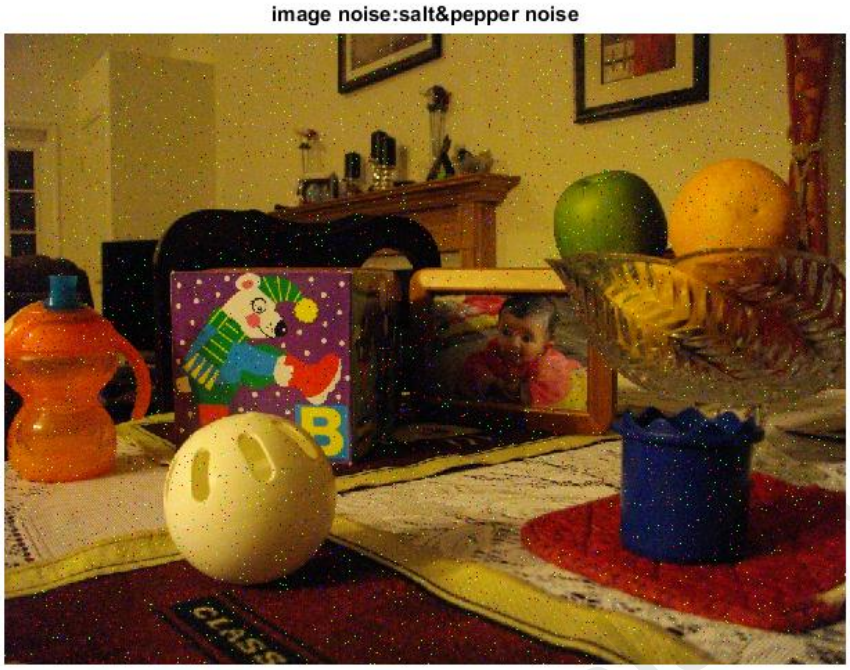

Figure 3.11 Salt and Pepper Noise (Density=0.01)

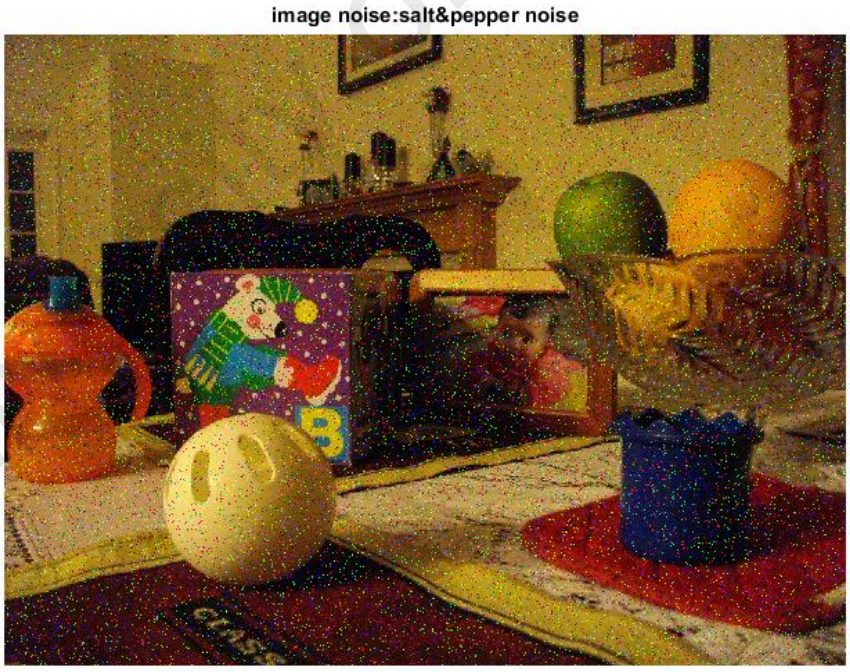

Figure 3.12 Salt and Pepper Noise (Density=0.05)

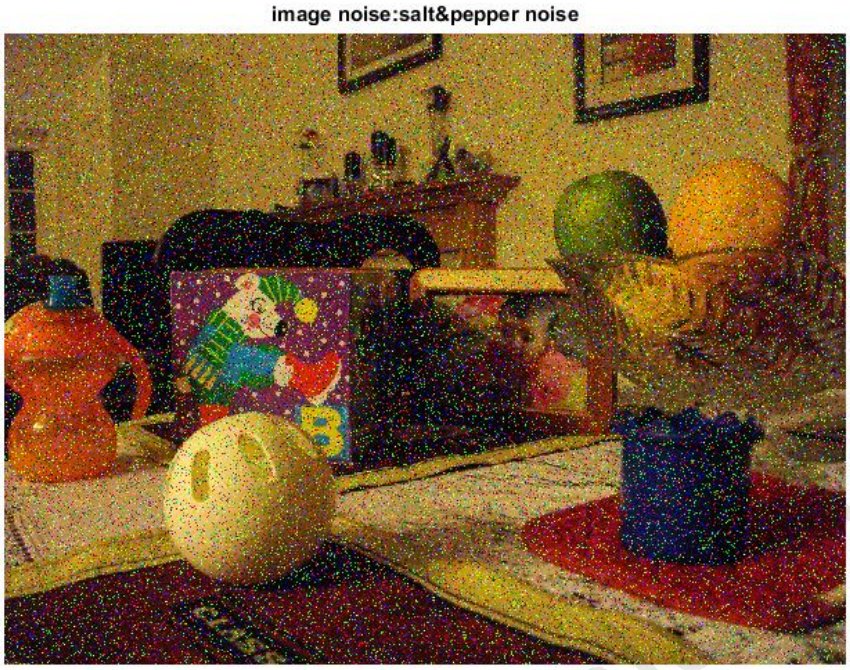

Figure 3.13 Salt and Pepper Noise (Density=0.01)

Figure 3.14 Salt and Pepper Noise (Density=0.5)

3.3 Image Quality Assessment (IQA)

Image Quality assessment plays an important role in various image processing applications. It is still an active area of research. A great deal of effort has been made in recent years to develop objective image quality metrics that correlate well with perceived human quality measurement or subjective methods. Objective image quality metrics can be categorized into three different classes, namely full reference, reduced reference, and no reference, depending on the availability of the original image with which the restored image is to be compared with (Varnan et al., 2012). In this work, the full reference (FR) approach were derived based on pixel to pixel error such as mean square error(MSE) or peak signal to noise ratio(PSNR), structural similarity index metric(SSIM). These were applied in current study for evaluating and estimating the quality of distorted images.

3.3.1 Mean squared Error (MSE)

It stands for the mean squared difference between the original image and distorted image. The mathematical definition for MSE (Eskicioglu & Fisher, 1995).

$$\mathrm{MSE} = \left(\frac{1}{\mathrm{M} * \mathrm{N}}\right) \sum_{\mathrm{i}=1}^{\mathrm{M}} \sum_{\mathrm{j}=1}^{\mathrm{N}} (\mathrm{a_{ij}} - \mathrm{b_{ij}})^2$$

In Equation (3.1), a_{ij} means the pixel value at position (i,j) in the original image and b_{ij} means the pixel value at the same position in the corresponding distorted image.

3.3.2 Peak Signal-to-Noise Ratio (PSNR)

PSNR is a classical index defined as the ratio between the maximum possible power of a signal and the power of corrupting noise that affects the fidelity of its representation (Zhe & Wu, 2004).

$$\mathrm{PSNR} = 10\log_{10} 255^2 / \mathrm{MSE}$$

Where 255 is the maximal possible value the image pixels when pixels are represented using 8 bits per sample, and MSE (mean square error) is the Euclidian distance between the original and the degraded images. The major advantages of these metrics are its simplicity and mathematical tractability, but they are not correlating well with perceived quality measurement because the Human Vision System characteristics are not considered in their models. PSNR is more consistent in the presence of noise compared to the SNR. By using the CSF (contrast sensitivity function) as the weighting function, we can define weighted SNR (WSNR) as the ratio of the average weighted signal power to the average weighted noise power.

3.3.3 Structural Similarity Index (SSIM)

is a full reference metric, or we can say the measuring of image quality based on an initial uncompressed or distortion-free image as reference. It compares two images using information about luminous, contrast and structural functions between the two input images (Li & Bovik, 2010). The luminous, contrast and structure function of the SSIM index are formulated individual as follows (Kudelka, 2012).

$$\text{luminous}, l(x,y) = \frac{2m_x m_y + C_1}{2m_x^2 + m_y^2 + C_1}$$

$$\text{contrast}, c(x,y) = \frac{2\sigma_x \sigma_y + C_2}{2\sigma_x^2 + \sigma_y^2 + C_2}$$

$$\text{structural}, s(x,y) = \frac{\sigma_{xy} + C_3}{\sigma_x \sigma_y + C_3}$$

where m_x and m_y represent the means of original image and restored image, respectively; $\sigma_x$and $\sigma_y$are standard deviation of original image and restored image, respectively; $\sigma_{xy}$is the covariance between original image and restored image; $C_1, C_2 \text{and } C_3$are constants that stabilized the computation when the denominators

become small. The combination of the luminous, contrast and structural functions yields a general form of SSIM index as follows:

$$\text{SSIM}\ (x,y) = \frac{(2m_x m_y + C_1)(2\sigma_{xy} + C_2)}{(m_x^2 + m_y^2 + C_1)(\sigma_x^2 + \sigma_y^2 + C_2)}$$

SSIM index is a maximum (1) if only the original image equates restored image (Dosselmann & Yang, 2008).

3.4 Image restoration techniques

3.4.1 Direct Inverse Filter

Direct inverse filter computes an optimal estimate $\hat{F}(u,v)$ of the original image F(u,v) simply dividing the degraded image G(u,v) by the degradation function H(u,v)as follows:

$$\hat{F}(u,v) = \frac{G(u,v)}{H(u,v)}$$

Substitute $G(u,v)$with F(u,v) H(u,v)+N(u,v):

$$\hat{F}(u,v) = \frac{F(u,v)H(u,v) + N(u,v)}{H(u,v)}$$

$$\hat{F}\ (u,v) = \frac{F(u,v)H(u,v)}{H(u,v)} + \frac{N(u,v)}{H(u,v)}$$

$$\hat{F}(u,v) = F(u,v) + \frac{N(u,v)}{H(u,v)}$$

It is interesting to note that the direct inverse filter can recover a degraded image exactly in the absence of noise. However, in the event that the noise is unknown, then it is impossible for a direct inverse filter to reconstruct the degraded image. Furthermore,

in the event that the degradation function has zero or absolute small values, then the noise can easily dominate the estimate - $\hat{F}(u,v)$.

In a nutshell, the direct inverse filter makes no explicit for managing noise and tends to allow noise to dominate over the estimate in the process of restoration.

3.4.2 Wiener Filter

The direct inverse filter is a poor image restoration technique in general and particularly vulnerable to noise. Therefore, Wiener filter is an enhanced image restoration technique that integrates not only the degradation function but also statistical properties of noise and original image in the reconstruction process.

Wiener filter obtains an optimal estimate $\hat{f}(x,y)$ of the original image $f(x,y)$ by minimizing the mean square error (MSE) between them on the assumption that the noise and the original image are uncorrelated. The detailed derivation of Weiner filter is as follows:

$$e^2 = E\left[\left|f(x,y) - \hat{f}(x,y)\right|^2\right]$$

$$e^2 = E[|f(x,y) - g(x,y) * w(x,y)|^2]$$

Convert the statistical error function to frequency domain by applying Fourier transform onto each the corresponding terms:

$$e^2 = E[|F(u,v) - F(u,v)W(u,v)|^2]$$

Apply $G(u,v) = F(u,v)H(u,v) + N(u,v)$ into the statistical error function above to obtain:

$$e^2 = E[|F(u,v) - (F(u,v)H(u,v) + N(u,v))W(u,v)|^2]$$

$$e^2 = E[|F(u,v) - F(u,v)H(u,v)W(u,v) - N(u,v))W(u,v)|^2]$$

$$e^2 = E[|F(u,v)(1 - W(u,v)H(u,v)) - N(u,v)W(u,v)|^2]$$

Apply complex conjugate formula, $|z|^2 = z\bar{z} = z\bar{z}$:

$$e^2 = E\big[(F(u,v)\big(1 - W(u,v)H(u,v)\big) - N(u,v)W(u,v))\overline{(F(u,v)(1 - W(u,v)H(u,v)) - N(u,v)W(u,v))}\big]$$

$$e^2 = E\Big[\Big(F(u,v)\big(1 - W(u,v)H(u,v)\big) - N(u,v)W(u,v)\Big)\,\overline{(F(u,v)}\,\overline{\big(1 - W(u,v)H(u,v)\big)} - \overline{N(u,v)W(u,v)}\,\Big]$$

$$e^2 = E\Big[\Big(F(u,v)\overline{F(u,v)}\big(1 - W(u,v)H(u,v)\big)\overline{\big(1 - W(u,v)H(u,v)\big)} - F(u,v)\big(1 - W(u,v)H(u,v)\big)\overline{N(u,v)W(u,v)} - \overline{(F(u,v)}\overline{\big(1 - W(u,v)H(u,v)\big)}N(u,v)W(u,v) + W(u,v)\overline{W(u,v)}\,N(u,v)\overline{N(u,v)}\Big)\Big]$$

The noise, $N(u,v)$ is assumed to be independent of the original image $F(u,v)$, hence:

$$E\big[\overline{F(u,v)}\,F(u,v)\big] = E\big[\overline{N(u,v)}\,F(u,v)\big] = 0$$

Apply the assumption that the noise and the original image are uncorrelated into the statistical error function:

$$e^2 = E\Big[F(u,v)\overline{F(u,v)}\big(1 - W(u,v)H(u,v)\big)\overline{\big(1 - W(u,v)H(u,v)\big)} + W(u,v)\overline{W(u,v)}\,N(u,v)\overline{N(u,v)}\;\Big]$$

In addition, the power spectral densities of the noise and original image are defined as follows:

$$S_F(u,v) = |F(u,v)|^2$$

$$S_N(u,v) = |N(u,v)|^2$$

Therefore,

$$e^2 = E\left[S_F(u,v)\left(1 - W(u,v)H(u,v)\right)\overline{\left(1 - W(u,v)H(u,v)\right)} + W(u,v)\overline{W(u,v)}\, S_N(u,v)\right]$$

Find the minimum value of the function by differentiating the statistical error function with respect to Wiener filter, $W(u,v)$:

$$\frac{d\varepsilon}{dW} = -H(u,v)\overline{\left(1 - W(u,v)H(u,v)\right)}S_F(u,v) + \overline{W(u,v)}\, S_N(u,v)$$

$$\frac{d\varepsilon}{dW} = \overline{W(u,v)}\, S_N(u,v) - H(u,v)\overline{\left(1 - W(u,v)H(u,v)\right)}S_F(u,v)$$

Set derivative equal to zero and solve for wiener filter, $W(u,v)$:

$$\overline{W(u,v)}\, S_N(u,v) - H(u,v)\overline{\left(1 - W(u,v)H(u,v)\right)}S_F(u,v) = 0$$

$$\overline{W(u,v)}\, S_N(u,v) = H(u,v)\overline{\left(1 - W(u,v)H(u,v)\right)}S_F(u,v)$$

$$\overline{W(u,v)}\, S_N(u,v) = S_F(u,v)\, H(u,v) - S_F(u,v)\, H(u,v)\overline{H(u,v)W(u,v)}$$

$$S_N(u,v) = \frac{S_F(u,v)H(u,v)}{\overline{W(u,v)}} - \frac{S_F(u,v)\, H(u,v)\overline{H(u,v)W(u,v)}}{\overline{W(u,v)}}$$

$$S_N(u,v) = \frac{S_F(u,v)H(u,v)}{\overline{W(u,v)}} - S_F(u,v)\,H(u,v)\overline{H(u,v)}$$

$$S_N(u,v) + S_F(u,v)\,H(u,v)\overline{H(u,v)} = \frac{S_F(u,v)H(u,v)}{\overline{W(u,v)}}$$

$$\overline{W(u,v)} = \frac{S_F(u,v)H(u,v)}{S_N(u,v) + S_F(u,v)\,H(u,v)\overline{H(u,v)}}$$

$$\overline{W(u,v)} = \frac{S_F(u,v)H(u,v)}{S_N(u,v) + S_F(u,v)\,H(u,v)\overline{H(u,v)}} \times \frac{\frac{1}{\overline{S_F(u,v)}}}{\frac{1}{\overline{S_F(u,v)}}}$$

$$\overline{W(u,v)} = \frac{H(u,v)}{\frac{S_N(u,v)}{\overline{S_F(u,v)}} + H(u,v)\overline{H(u,v)}}$$

$$W(u,v) = \frac{\overline{H(u,v)}}{\frac{S_N(u,v)}{\overline{S_F(u,v)}} + H(u,v)\overline{H(u,v)}}$$

$$W(u,v) = \frac{\overline{H(u,v)}}{\frac{S_N(u,v)}{\overline{S_F(u,v)}} + H(u,v)\overline{H(u,v)}} \times \frac{H(u,v)}{H(u,v)}$$

$$W(u,v) = \frac{\overline{H(u,v)}H(u,v)}{\frac{S_N(u,v)}{\overline{S_F(u,v)}} + H(u,v)\overline{H(u,v)}} \times \frac{1}{H(u,v)}$$

$$W(u,v) = \frac{|H(u,v)|^2}{\frac{S_N(u,v)}{\overline{S_F(u,v)}} + |H(u,v)|^2} \times \frac{1}{H(u,v)}$$

$$\hat{F}(u,v) = W(u,v) \times G(u,v)$$

$$\hat{F}(u,v) = \left[\frac{|H(u,v)|^2}{\frac{S_N(u,v)}{S_F(u,v)} + |H(u,v)|^2} \times \frac{1}{H(u,v)}\right] \times G(u,v)$$

where

$\hat{F}(u,v)$ = optimal estimate of original image $F(u,v)$

$H(u,v)$ = the degradation/blurring/PSF/OTF function

$|H(u,v)|^2 = \overline{H(u,v)}\, H(u,v)$

$\overline{H(u,v)}$ = the complex conjugate of $H(u,v)$

$S_F(u,v) = |F(u,v)|^2$ = the power spectrum of the original image

$S_N(u,v) = |N(u,v)|^2$= the power spectrum of the additive noise

Power spectrum density (PSD) or power spectrum of a signal describes the average signal power per spatial frequency (u,v). The power spectral densities of original image and additive noise are represented by $S_F(u,v)$ and $S_N(u,v)$ respectively.

The ratio $S_N(u,v)/S_F(u,v)$ is known as the noise to signal power ratio. It is important to note that in the absence of noise, the power spectrum of noise, $S_N(u,v)$ is zero, hence, the noise to signal power ratio becomes zero as well. In other words, the Wiener filter reduces or approximates to a direct inverse filter in the absence of noise.

Furthermore, the power spectrum of the noise is determined by the noise variance only for all spatial frequencies due to the assumption that the noise is independent of the original Image, thus has zero mean.

$$S_N(u,v) = \sigma^2 \text{for all } (u,v)$$

However, the estimation of power spectrum of the original image is often challenging since the original image in practical case is obviously unavailable. Thus, period gram is an approach commonly used to estimate the power spectrum of the original image by determining the power spectrum of the degraded image and compensating for the variance of the noise σ_n^2.

$$S_F(u,v) \approx S_G(u,v) - \sigma_n^2 \approx \frac{1}{NM}\overline{G(u,v)}G(u,v) - \sigma_n^2$$

Last but not least, it is important to note that even in the event that the noise to signal power ratio is unknown, the optimal estimate of the original image can still be obtained by varying the constant ratio and observing the restored outcomes.

3.4.3 Wavelet Transform Filter

A wavelet is a function corresponding to a small oscillation, hence its name. Used in wavelet decomposition, decomposition like short-term Fourier transform, used in signal processing.

In mathematics, a wavelet ψ is a summable square function of the Hilbert space defined as: $\forall t \in \mathbb{R}, \psi_{s,\tau}(t) = \frac{1}{\sqrt{s}}\psi\left(\frac{t-\tau}{s}\right)$

where: $(s,t) \in \mathbb{R}^{+*} \times \mathbb{R}$

3.4.3.1 Discrete wavelets transform (DWT)

Analyzing assumable square wavelet function consists in calculating all its scalar products. The obtained numbers are called wavelet coefficients, and the operation associating a function with its wavelet coefficients is called a wavelet transform. We can adapt the wavelet transform in the case where we are in a discrete set. It is then a question of sampling the signal s on a dyadic scale and τ, thus:

$$\psi_{m,n}[t] = s_0^{-m/2}\psi(s_0^{-m}t - nT_0$$

In the case where the $\psi_{m,n}$form a Hilbert basis space, (this is the case, for example, of the Haar wavelet), the wavelet decomposition of a signal g consists in calculating the scalar products $(g, \psi_{m,n})$. The reconstruction of the signal is then obtained by:

$$g = \sum_{m\in Z}\sum_{m\in Z}(g, \psi_{m,n})\psi_{m,n}$$

The main disadvantages of the DWT are lack of directionality and shift-sensitivity (an unpredictable change in the output coefficients happens when the input signal shifts).

3.4.3.2 Dual -Tree Complex Wavelet Transform (DT-CWT)

The DT-CWT solves all the problems of the DWT as it is quasi shift-invariant and has a good directional selectivity. As shown in Figure 4.2, the same step function is applied as input signals with different phases to both DWT and DTCWT. The result is that, the coefficients of the DTCWT transform are less affected by the shift.

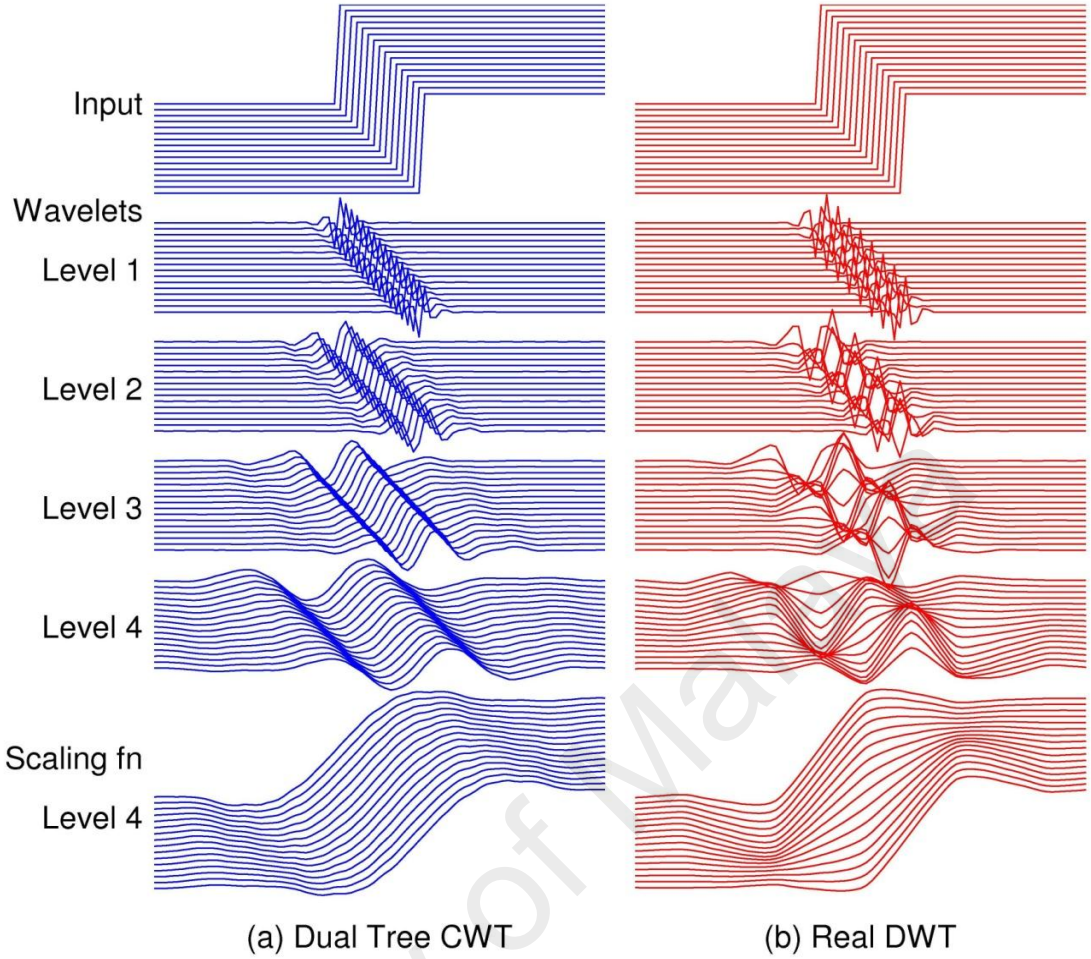

Figure 3.15 shifted step responses of both DWT and DTCWT.

As shown in the Figure 4.2 The DTCWT of a signal X(t) is calculated by means of two separate DWTs in parallel on the same data. Each tree has four levels (level 1 to 4 and of the level 4 scaling function). And each tree represents the real or the imaginary parts of the transform.

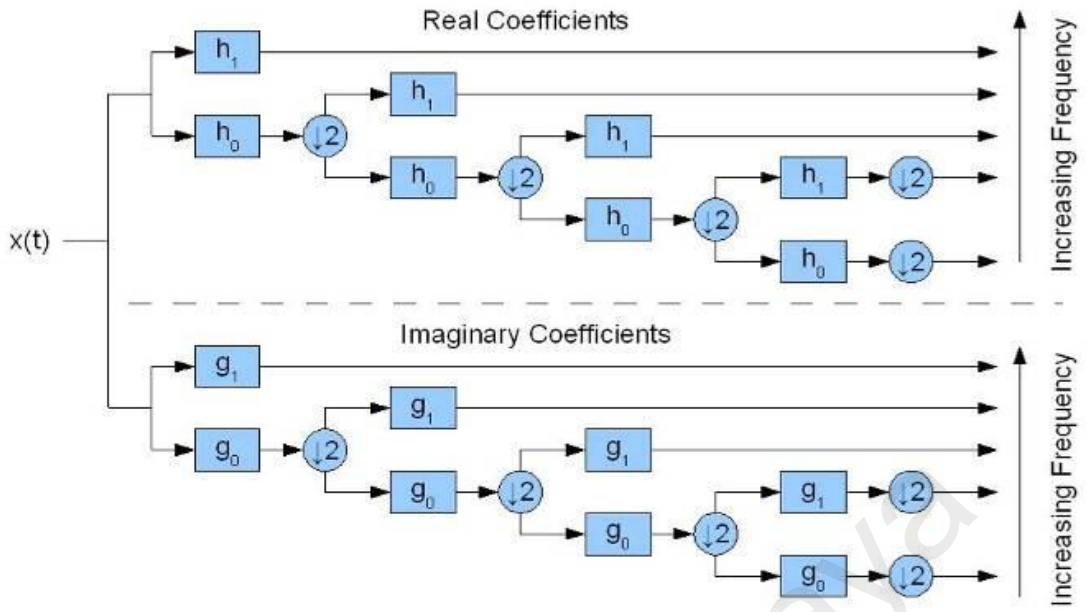

Figure 3.16 DTCWT implementation of a signal x.

CHAPTER 4: RESULTS AND DISCUSSION

This chapter shows the results of the three methods used to restore the degraded noise image. The restored image is evaluated using the image quality metrics discussed in the earlier chapters. A total of twelve images is used in this experimental study. The noise was added into images by using two methods are; Gaussian noise and Salt & Pepper.

4.1 Direct Inverse Filter

Figure 4.1 Restored image using Direct Inverse Filter in the absence of noise.

Direct inverse filter is mathematically formulated as follows:

$$\hat{F}(u,v) = \frac{F(u,v)H(u,v) + N(u,v)}{\mathrm{H}(u,v)}$$

However, in the absence of noise, the direct inverse filter reduces to:

$$\hat{F}(u,v) = \frac{F(u,v)H(u,v) + 0}{\mathrm{H}(u,v)}$$

$$\hat{F}(u,v) = \frac{F(u,v)\cancel{H(u,v)}}{\cancel{\mathrm{H}(u,v)}}$$

$$\hat{F}(u,v) = F(u,v)$$

Figure 5.1.1 elucidate and evaluate that a direct inverse filter is a suitable image restoration technique in the absence of noise. The MSE and PSNR of the resorted image in the absence of noise are 0.0003 and 84.0117, respectively. The MSE value indicates that the cumulative squared error between the restored image and the original image is extremely minimal whereas the high PSNR value indicates that the resorted image presents a high-quality image.

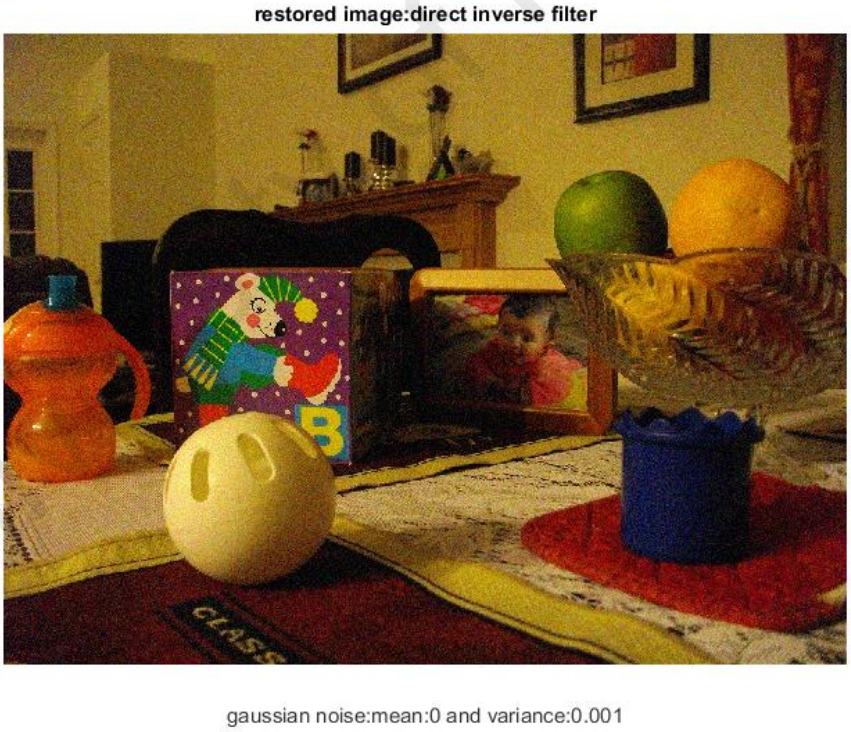

Figure 4.2 Restored Image using Direct Inverse Filter in the present of Gaussian noise with 0 mean and 0.001 variance.

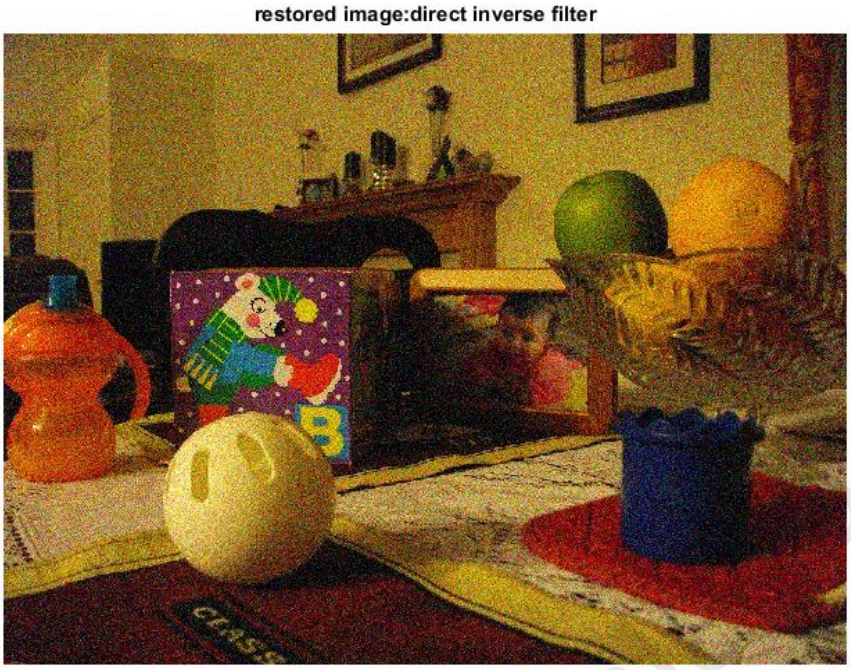

Figure 4.3 Restored Image using Direct Inverse Filter in the present of Gaussian noise with 0 mean and 0.005 variance.

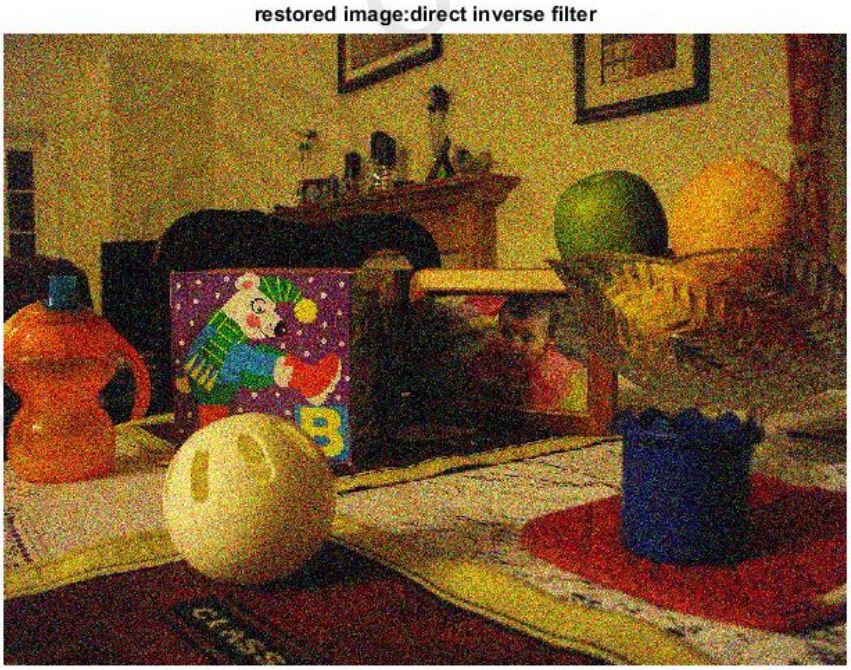

Figure 4.4 Restored Image using Direct Inverse Filter in the present of Gaussian noise with 0 mean and 0.01 variance.

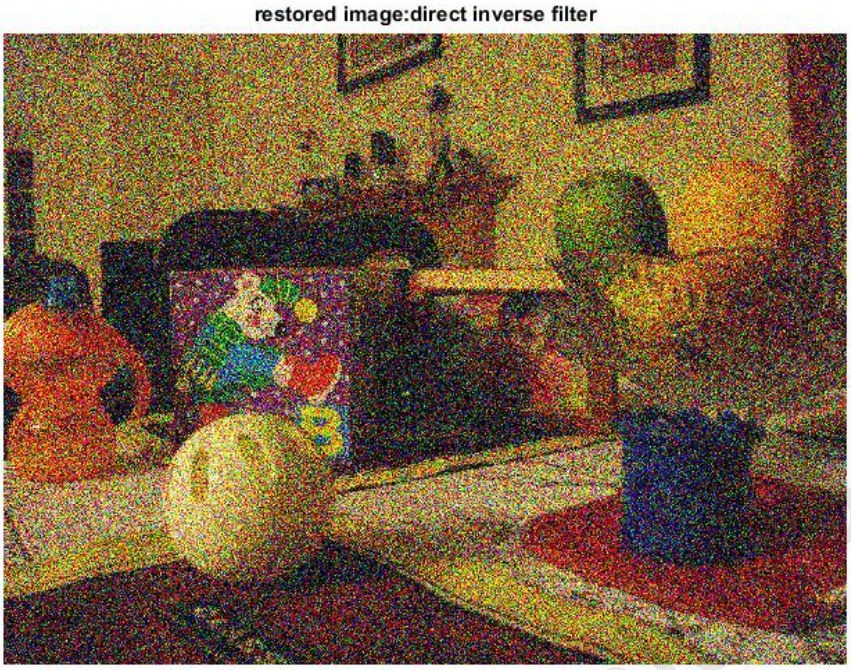

Figure 4.5 Restored Image using Direct Inverse Filter in the present of Gaussian noise with 0 mean and 0.05 variance.

Figure 4.6 Restored Image using Direct Inverse Filter in the present of Gaussian noise with 0 mean and 0.1 variance.

Figure 4.7 Restored Image using Direct Inverse Filter in the present of Gaussian noise with 0 mean and 0.5 variance.

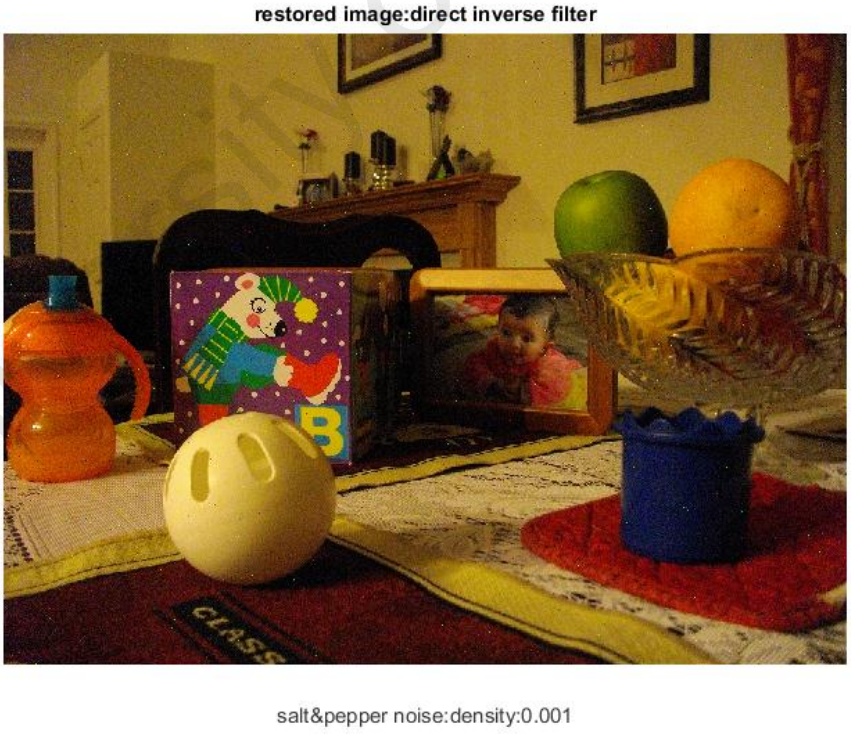

Figure 4.8 Restored Image using Direct Inverse Filter in the present of Salt &Pepper noise at 0.001 density.

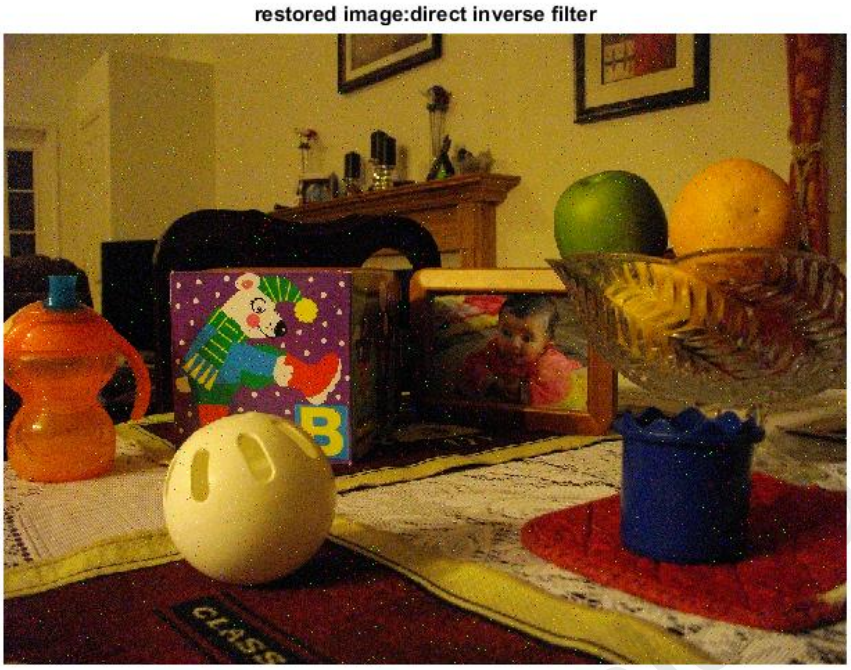

Figure 4.9 Restored Image using Direct Inverse Filter in the present of Salt &Pepper noise at 0.005 density.

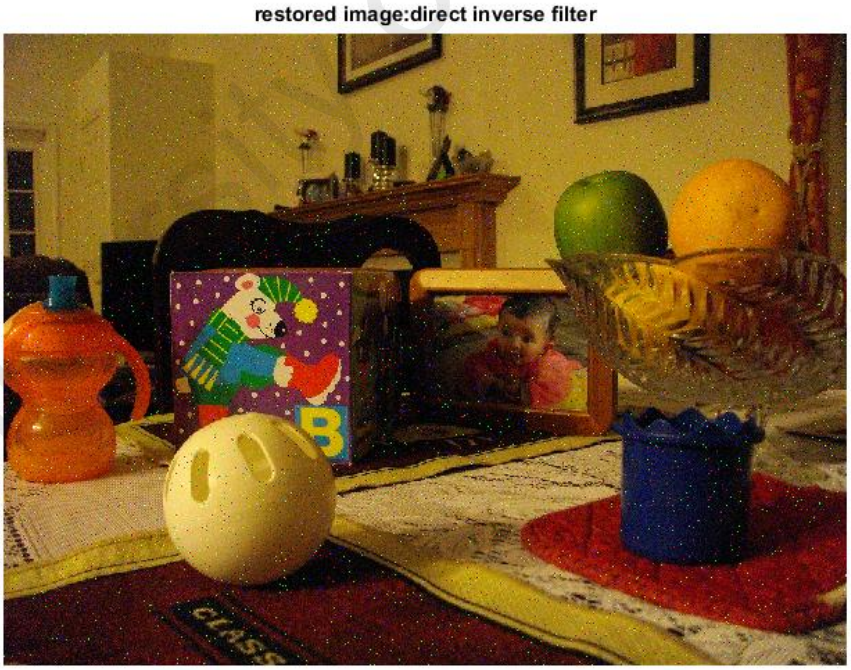

Figure 4.10 Restored Image using Direct Inverse Filter in the present of Salt &Pepper noise at 0.01 density.

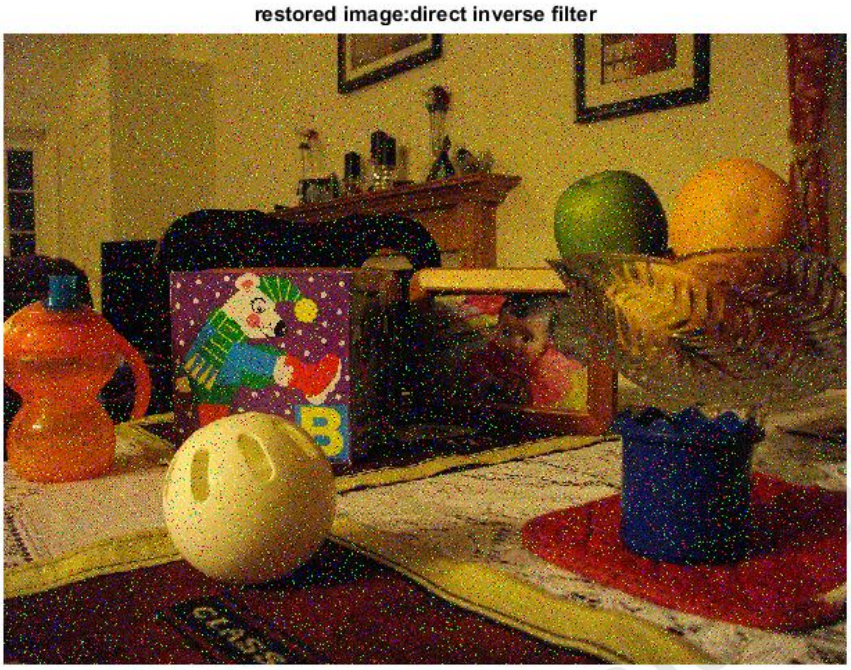

Figure 4.11 Restored Image using Direct Inverse Filter in the present of Salt &Pepper noise at 0.05 density

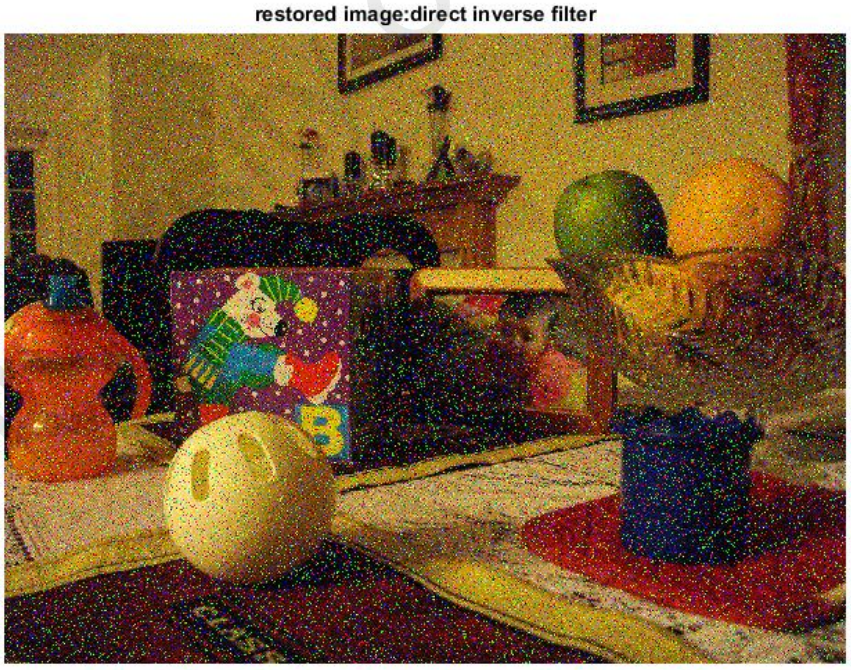

Figure 4.12 Restored Image using Direct Inverse Filter in the present of Salt &Pepper noise at 0.1 density.

Figure 4.13 Restored Image using Direct Inverse Filter in the present of Salt &Pepper noise at 0.5 density

Table 4.1 MSE, PSNR, and SSIM of Direct Inverse Filter

Direct Inverse Filter												
Quantitative Parameters	Gaussian Noise (Variance)						Salt & pepper Noise (Density)					
	0.001	0.005	0.01	0.05	0.1	0.5	0.001	0.005	0.01	0.05	0.1	0.5
MSE	0.0034	0.0144	0.0273	0.1140	0.1987	0.4938	0.0015	0.0061	0.0121	0.0578	0.1149	0.5212
PSNR (dB)	72.8596	66.5363	36.7735	57.5599	55.1498	51.1951	76.4053	70.2806	67.3145	60.5118	57.5288	50.9605
SSIM	0.6492	0.3465	0.2368	0.0803	0.0484	0.0178	0.8902	0.7595	0.6274	0.2300	0.1186	0.0200

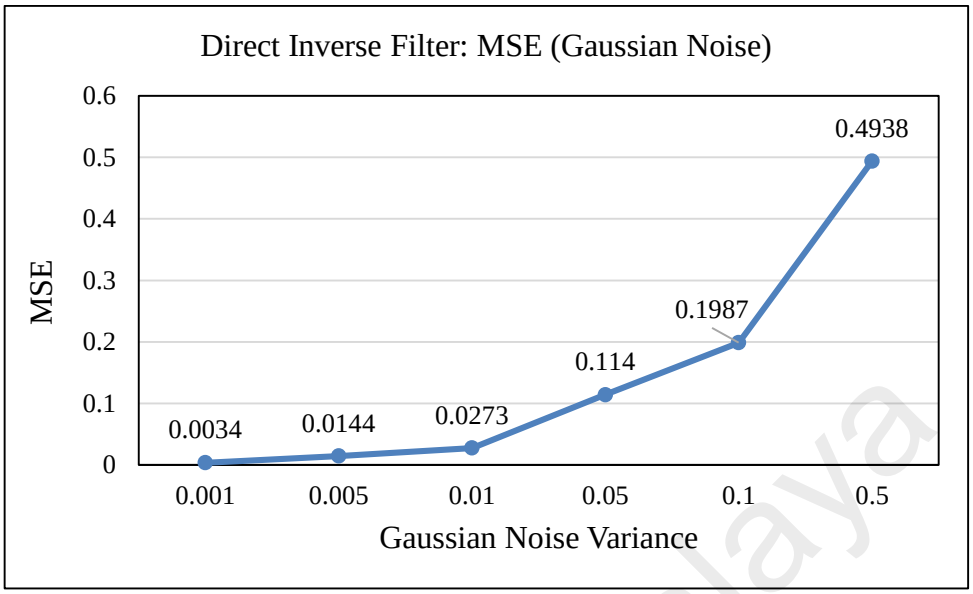

Figure 4.14 MSE of Direct Inverse Filter for Gaussian Noise.

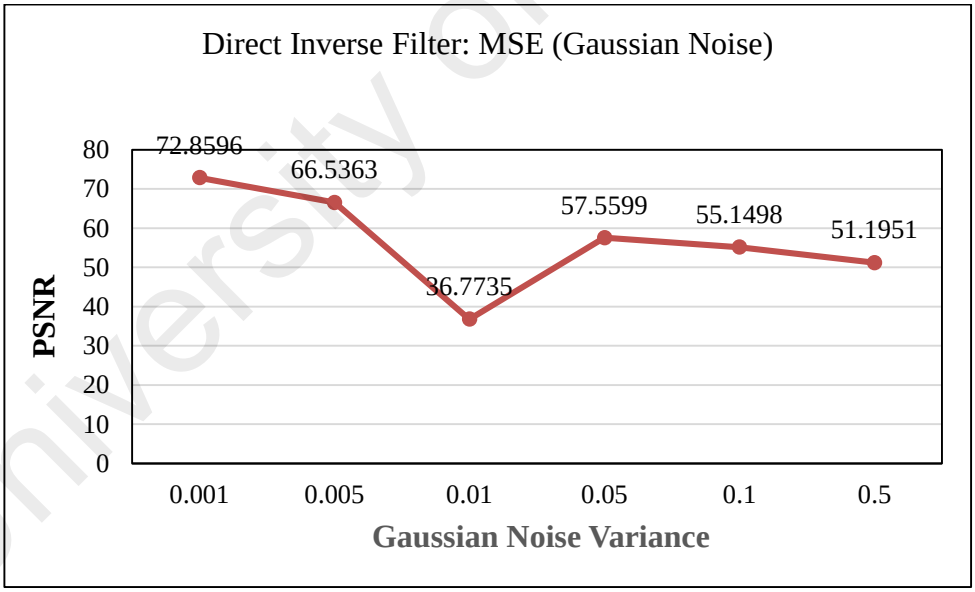

Figure 4.15 PSNR of Direct Inverse Filter for Gaussian Noise.

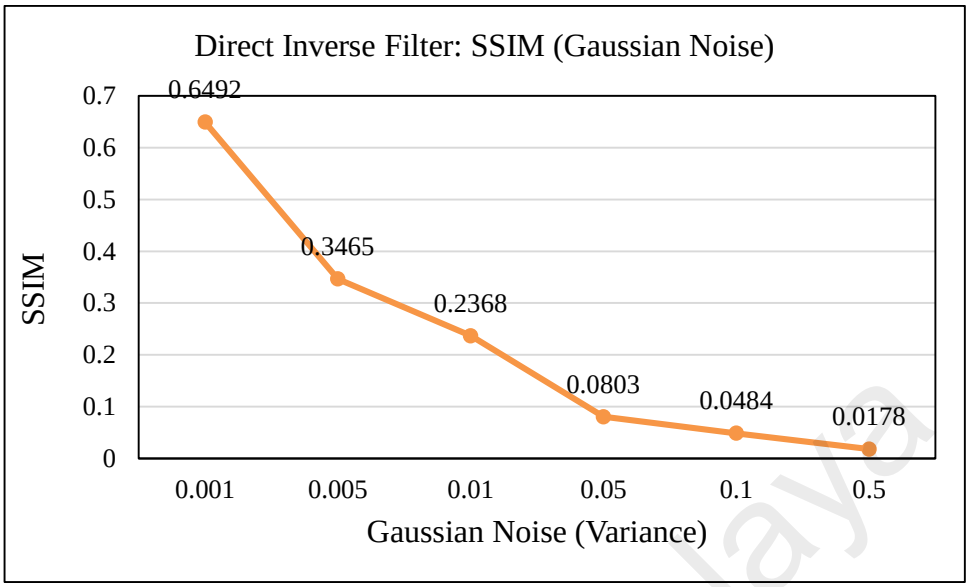

Figure 4.16 SSIM of Direct Inverse Filter for Gaussian Noise.

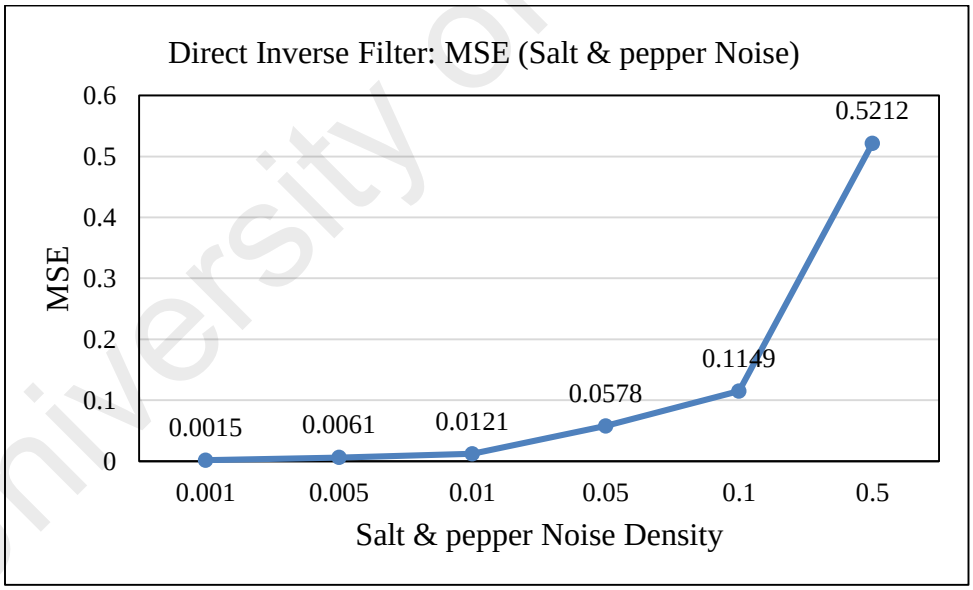

Figure 4.17 MSE of Direct Inverse Filter for Salt & Pepper Noise

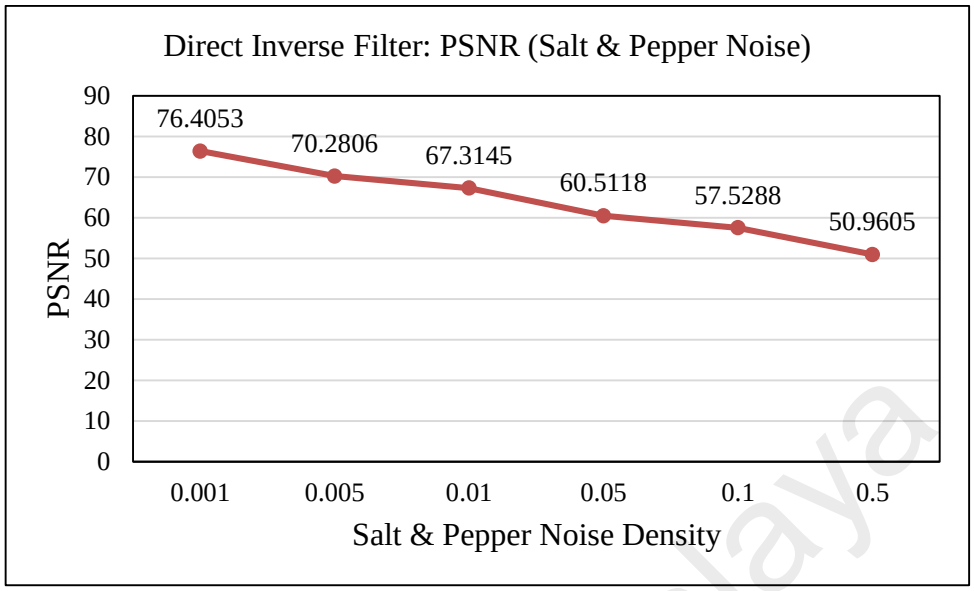

Figure 4.18 PSNR of Direct Inverse Filter for Salt & Pepper Noise

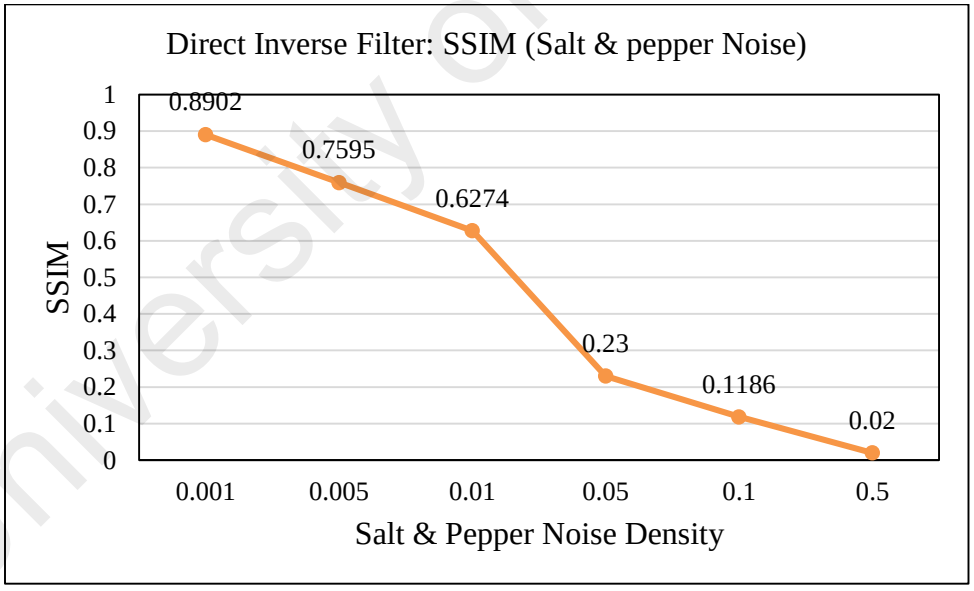

Figure 4.19 SSIM of Direct Inverse Filter for Salt & Pepper Noise

4.2 Wiener Filter

Weiner filter is mathematically formulated as follows:

$$\hat{F}(u,v) = \left[\frac{|H(u,v)|^2}{\frac{S_N(u,v)}{S_F(u,v)} + |H(u,v)|^2} \times \frac{1}{H(u,v)}\right] \times G(u,v)$$

where $\hat{F}(u,v)$ is the optimal estimate of original $F(u,v)$; $H(u,v)$ is the degradation function; $|H(u,v)|^2 = \overline{H(u,v)}H(u,v)$; $H(u,v)$ is the complex conjugate of $H(u,v)$; $S_F(u,v)=|F(u,v)|^2$ is the power spectrum of the original image; $S_N(u,v) = |N(u,v)|^2$ is the power spectrum of additive noise.

However, it is interesting to note that in the absence of noise, the noise to signal ratio, $S_N(u,v)/F(u,v)$ is zero and the Wiener filter reduces to a direct inverse filter as follows:

$$\hat{F}(u,v) = \left[\frac{|H(u,v)|^2}{0 + |H(u,v)|^2} \times \frac{1}{H(u,v)}\right] \times G(u,v)$$

$$\hat{F}(u,v) = \frac{G(u,v)}{H(u,v)}$$

Wiener filter has showed that the restored images are fairly closed to the original image although some noise is still obvious. Quantitatively, The MSE, PSNR, and SSIM methods are calculated and presented as illustrated in Table 5.2. They were applied for comparing and analyzing the quality between the restored images and the original image. Generally, the cumulative squared errors were achieved a very minimal value between the restored images and original image. Therefore, the qualities of the restored images were better. Thus, from Table 5.2 clearly showed that the noise increases, the cumulative error increases, and the quality of the restored image decreases.

Overall, although some noise is still shown, Wiener filter method generated restored image which it is closely like the original image by integrating the noise into signal ratio. However, the achievements of Wiener filter assume that the statistical properties of both noise and original image are recognized. Practically, one or more of these quantities is unrecognized, and the issue is that, the experimental signal to noise ratio should be repeated till an adequate result is achieved.

Figure 4.20 Restored Image using Wiener Filter in the present of Gaussian noise with 0 mean and 0.001 variance.

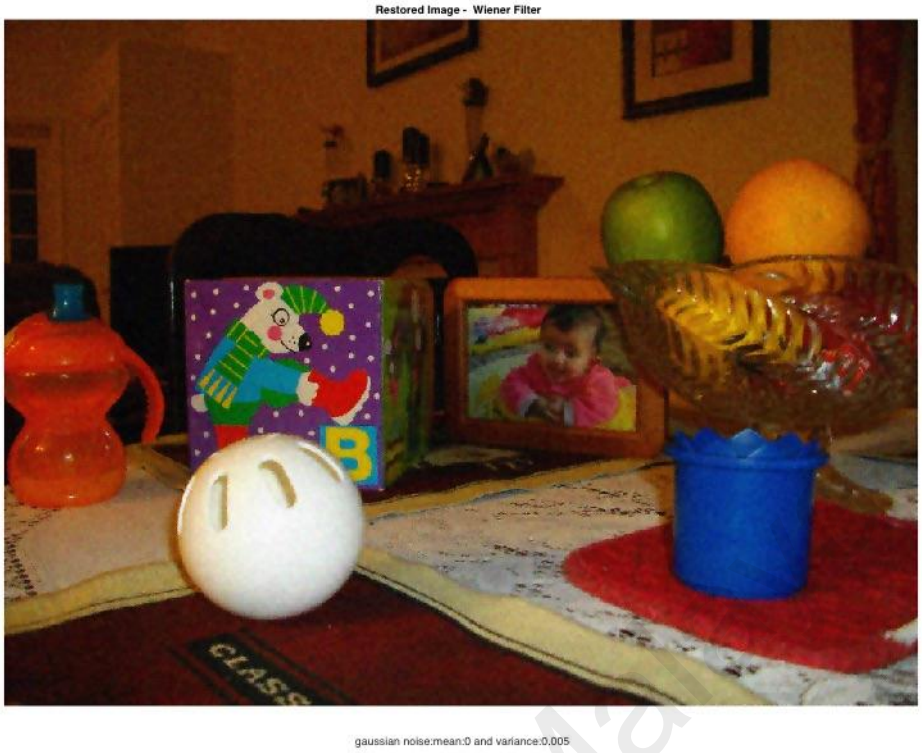

Figure 4.21 Restored Image using Wiener Filter in the present of Gaussian noise with 0 mean and 0.005 variance.

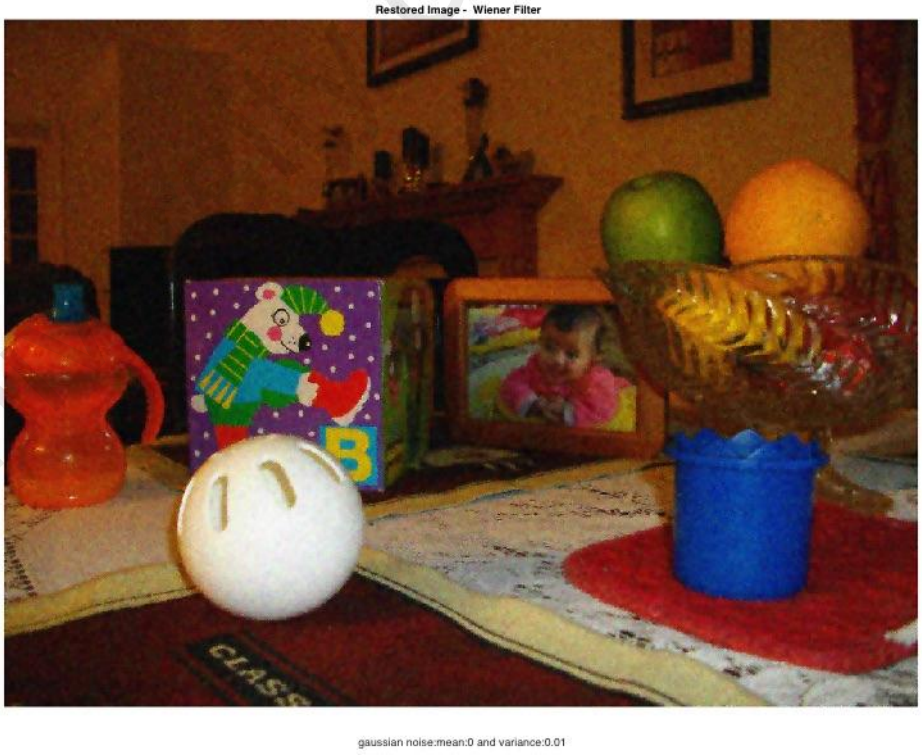

Figure 4.22 Restored Image using Wiener Filter in the present of Gaussian noise with 0 mean and 0.01 variance.

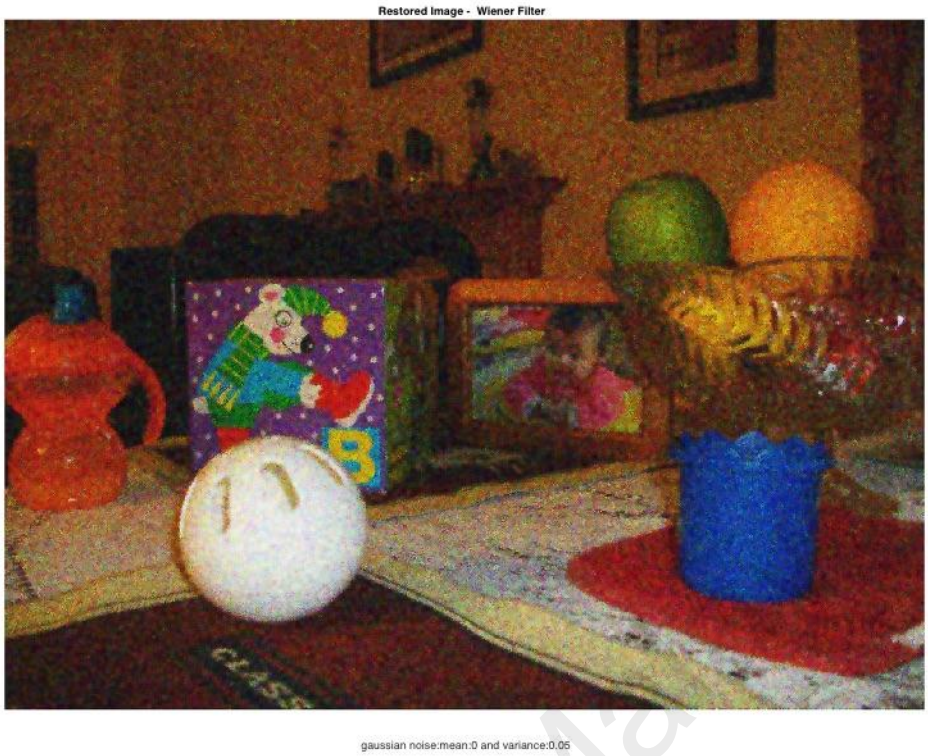

Figure 4.23 Restored Image using Wiener Filter in the present of Gaussian noise with 0 mean and 0.05 variance.

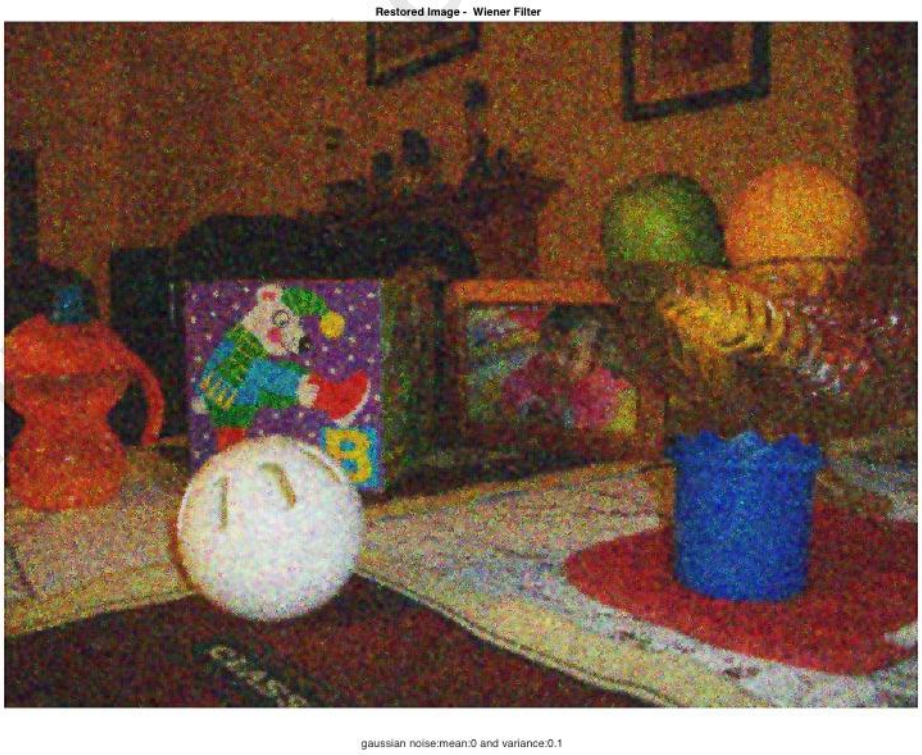

Figure 4.24 Restored Image using Wiener Filter in the present of Gaussian noise with 0 mean and 0.1 variance.

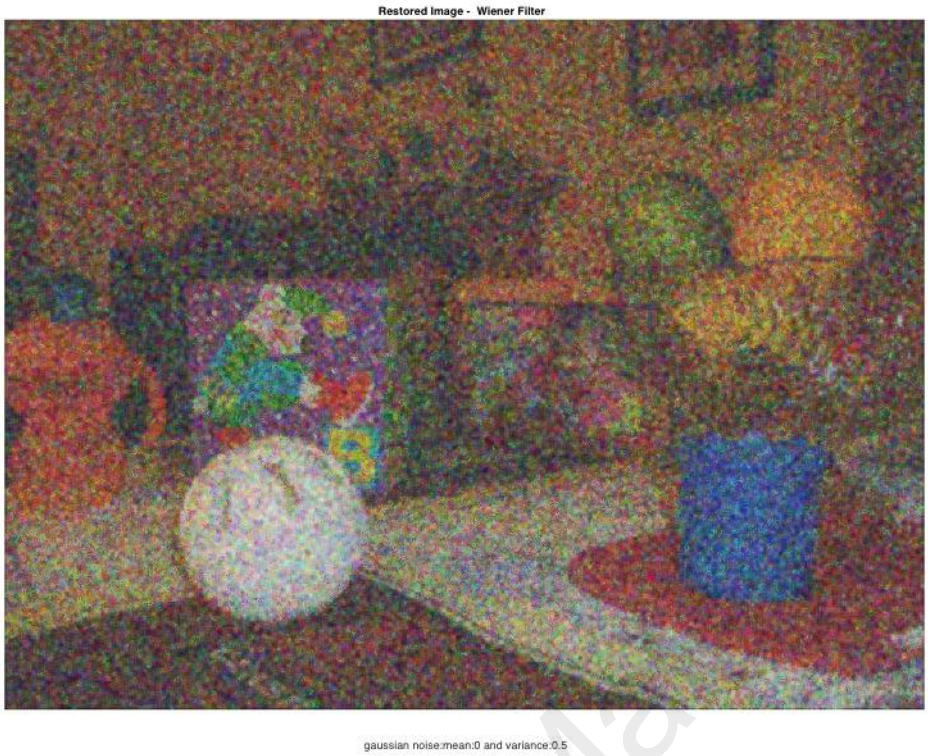

Figure 4.25 Restored Image using Wiener Filter in the present of Gaussian noise with 0 mean and 0.5 variance.

Figure 4.26 Restored Image using Wiener Filter in the present of Salt &Pepper noise at 0.001 density.

Figure 4.27 Restored Image using Wiener Filter in the present of Salt &Pepper noise at 0.005 density.

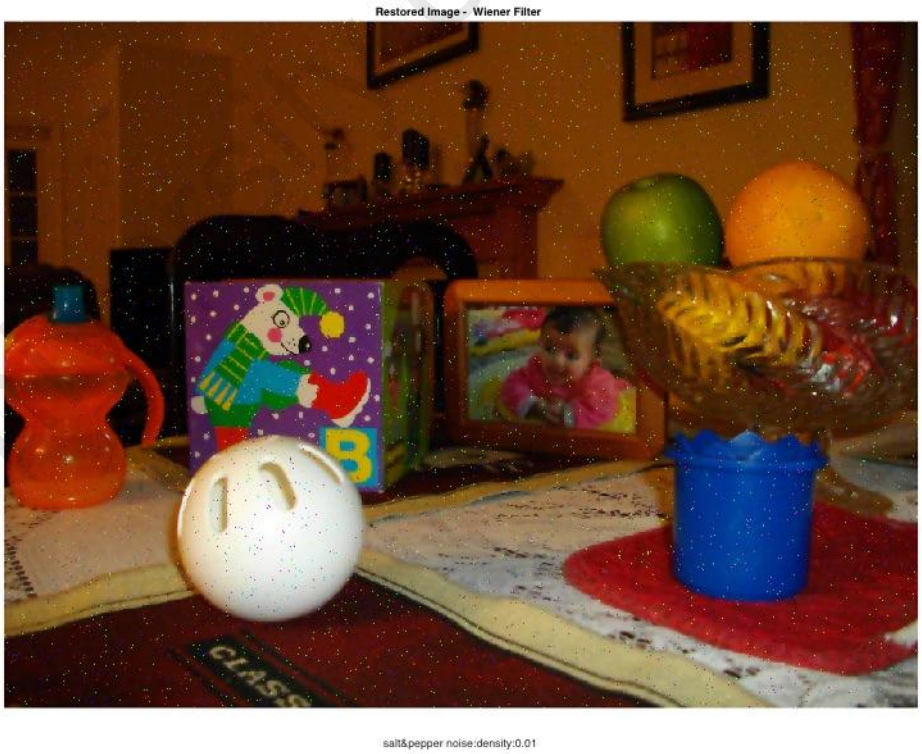

Figure 4.28 Restored Image using Wiener Filter in the present of Salt &Pepper noise at 0.01 density.

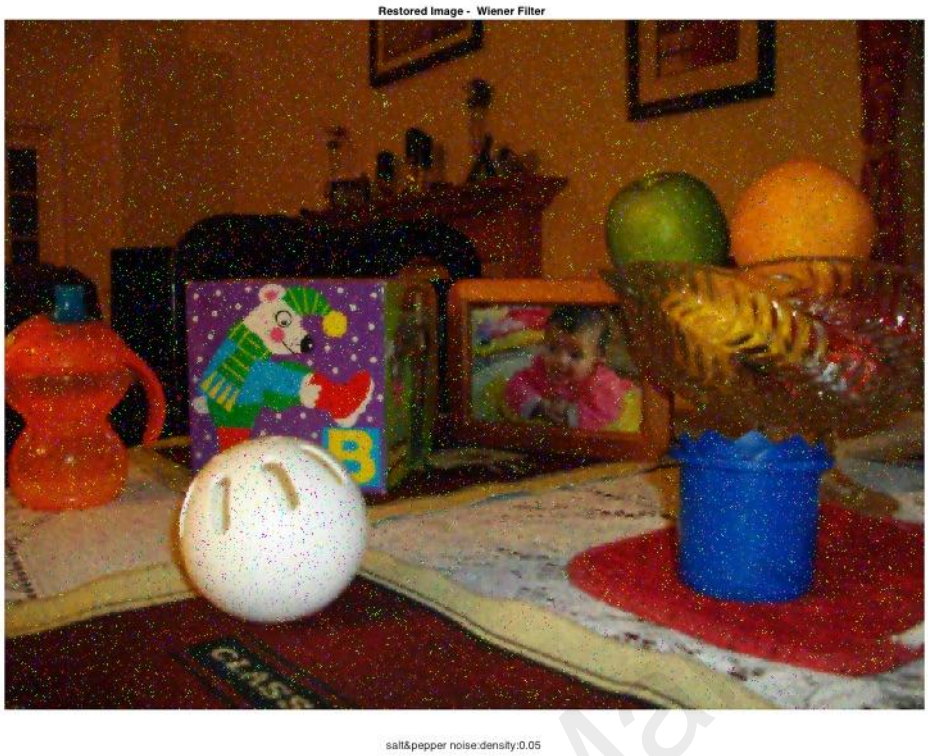

Figure 4.29 Restored Image using Wiener Filter in the present of Salt &Pepper noise at 0.05 density.

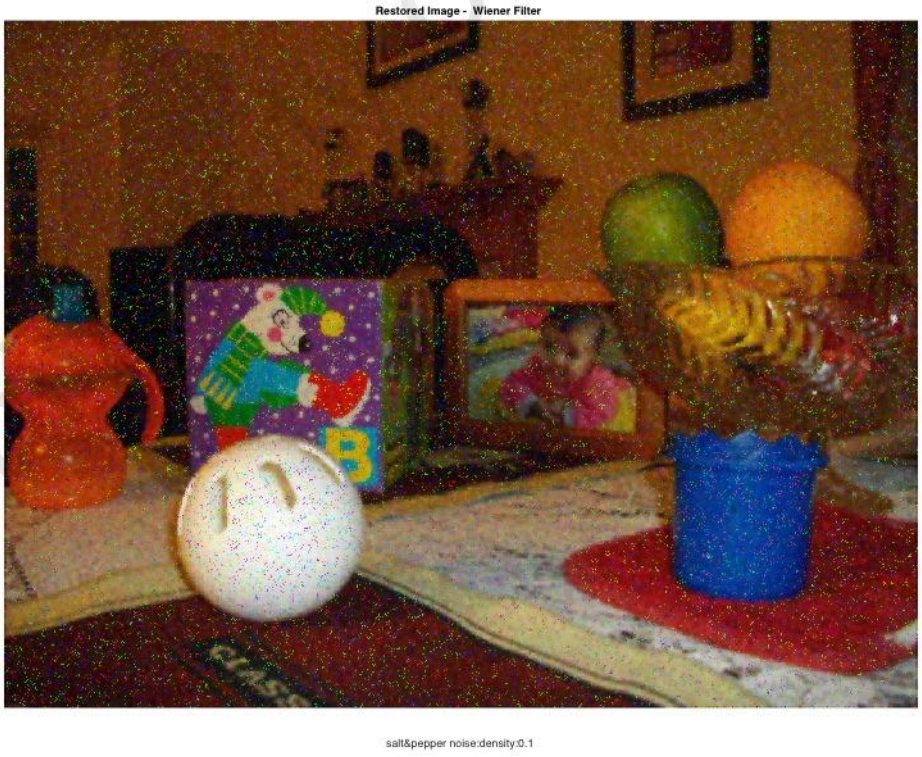

Figure 4.30 Restored Image using Wiener Filter in the present of Salt &Pepper noise at 0.1 density.

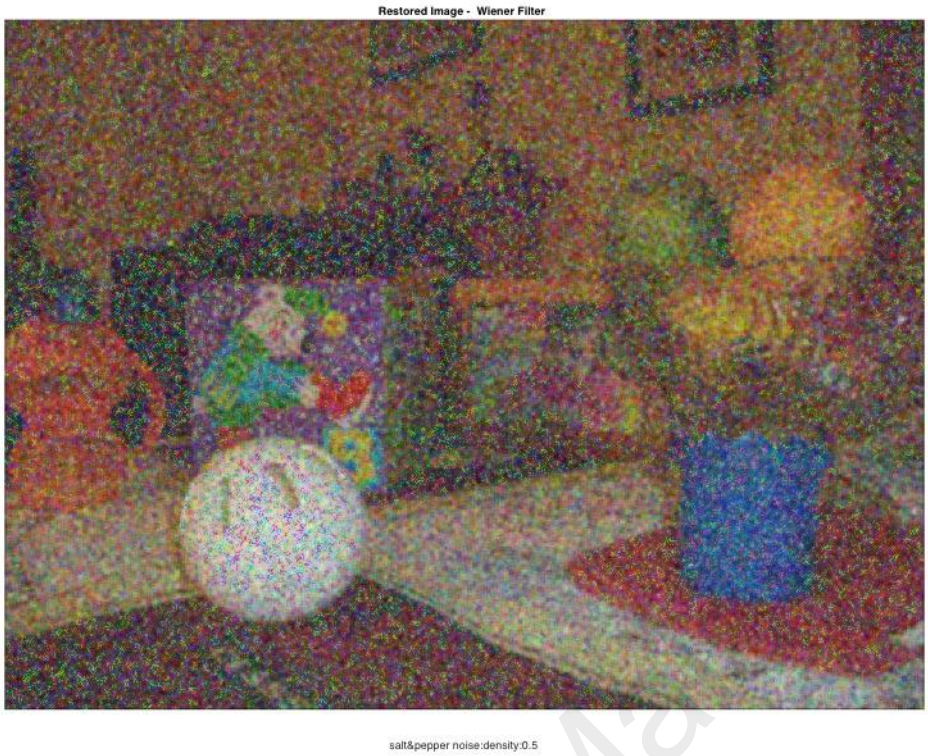

Figure 4.31 Restored Image using Wiener Filter in the present of Salt &Pepper noise at 0.5 density.

Table 4.2 MSE, PSNR, and SSIM of Wiener Filter

Wiener Filter												
Quantitative Parameters	**Gaussian Noise (Variance)**						**Salt & pepper Noise (Density)**					
	0.001	**0.005**	**0.01**	**0.05**	**0.1**	**0.5**	**0.001**	**0.005**	**0.01**	**0.05**	**0.1**	**0.5**
MSE	0.0003	0.0008	0.0015	0.0064	0.0119	0.0399	0.0005	0.0016	0.0027	0.0063	0.0088	0.0411
PSNR (dB)	82.8322	78.9040	76.4449	70.0626	67.3851	62.1160	80.9869	76.0517	73.7709	70.1169	68.7009	61.9916
SSIM	0.9738	0.9396	0.9057	0.7542	0.6537	0.4067	0.9718	0.9273	0.8851	0.7720	0.7223	0.4130

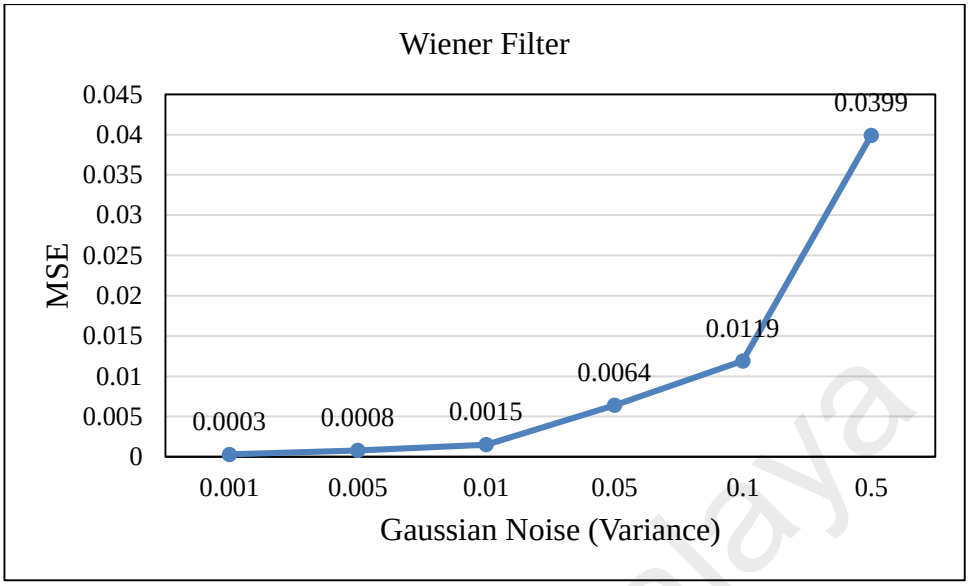

Figure 4.32 MSE of Wiener Inverse Filter for Gaussian Noise

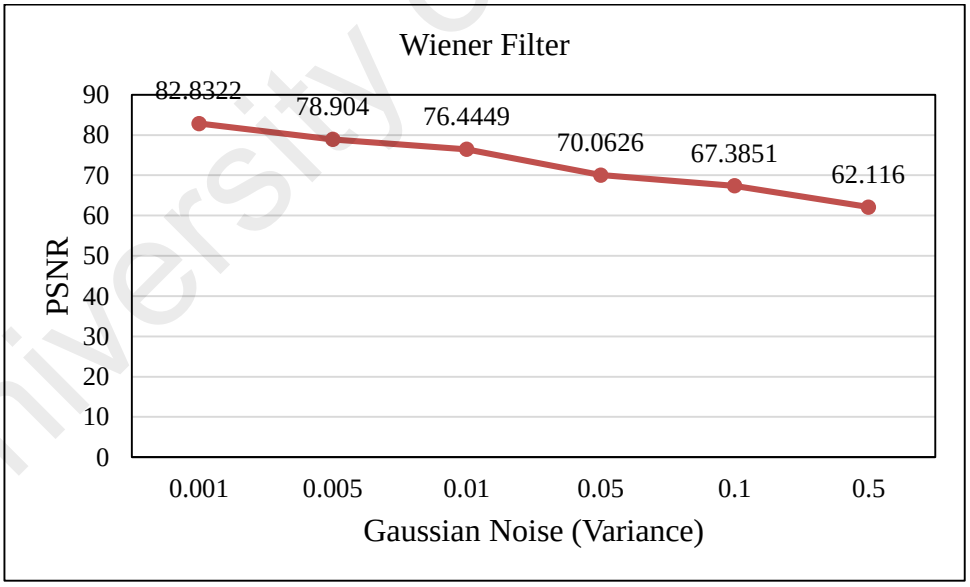

Figure 4.33 PSNR of Wiener Inverse Filter for Gaussian Noise

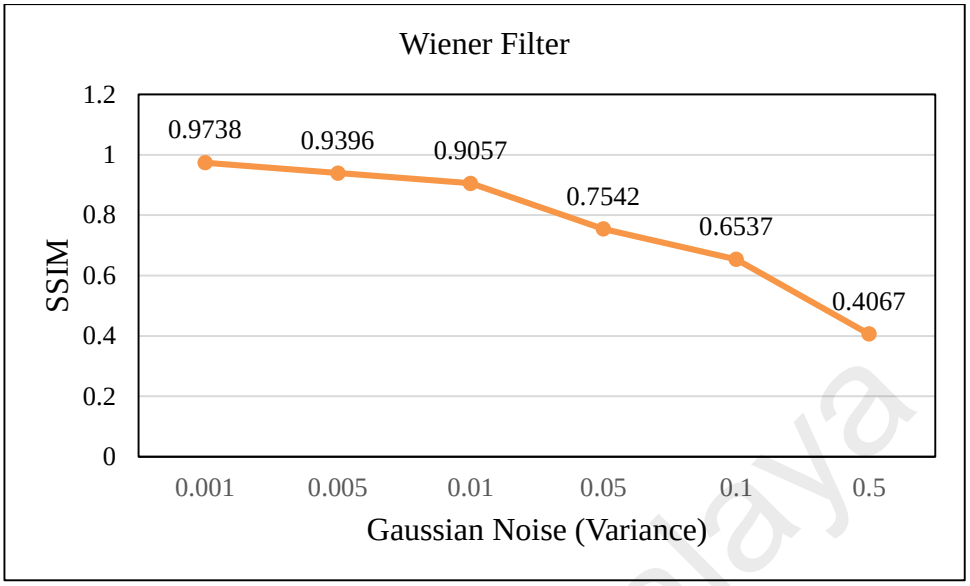

Figure 4.34 SSIM of Wiener Inverse Filter for Gaussian Noise

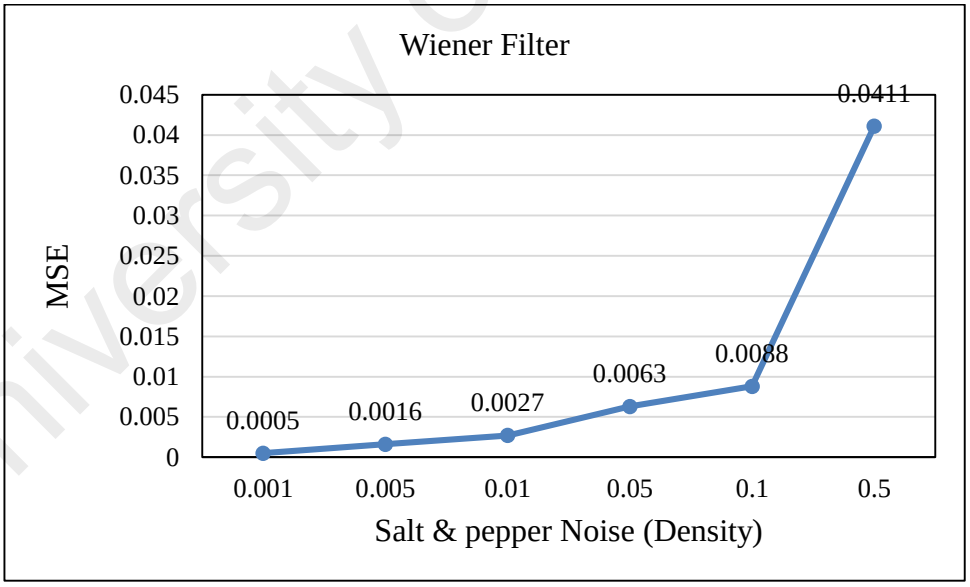

Figure 4.35 MSE of Wiener Inverse Filter for Salt & Pepper Noise

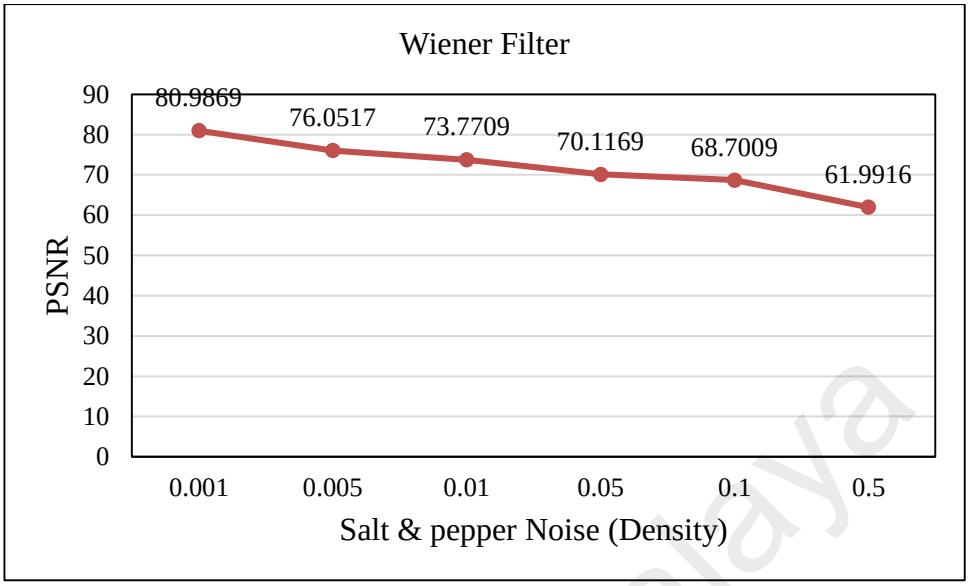

Figure 4.36 PSNR of Wiener Inverse Filter for Salt & Pepper Noise

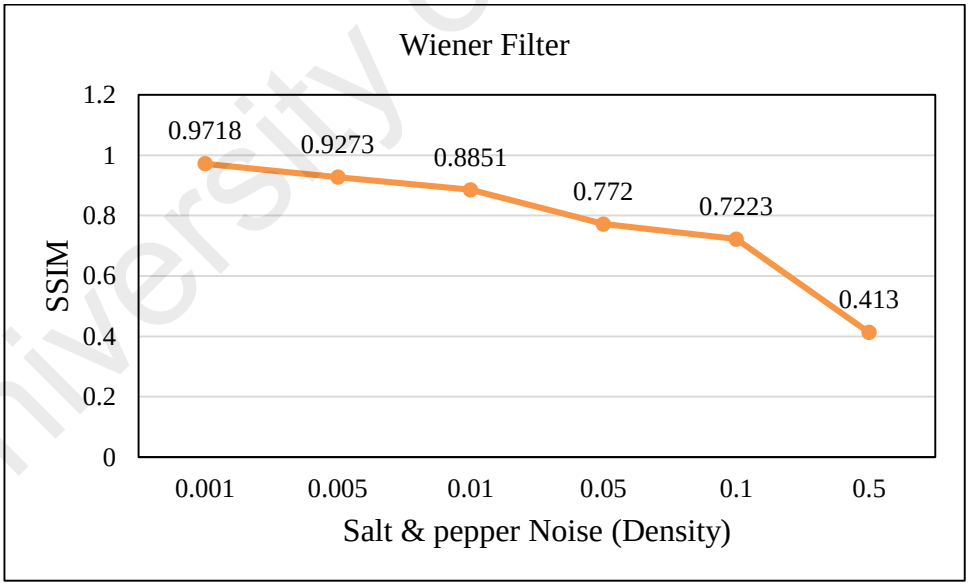

Figure 4.37 SSIM of Wiener Inverse Filter for Salt & Pepper Noise

4.3 Wavelet Transform Filter

Figure 4.38 Restored Image using Complex Dual Tree Wavelet Filter in the present of Gaussian noise with 0 mean and 0.001 variance.

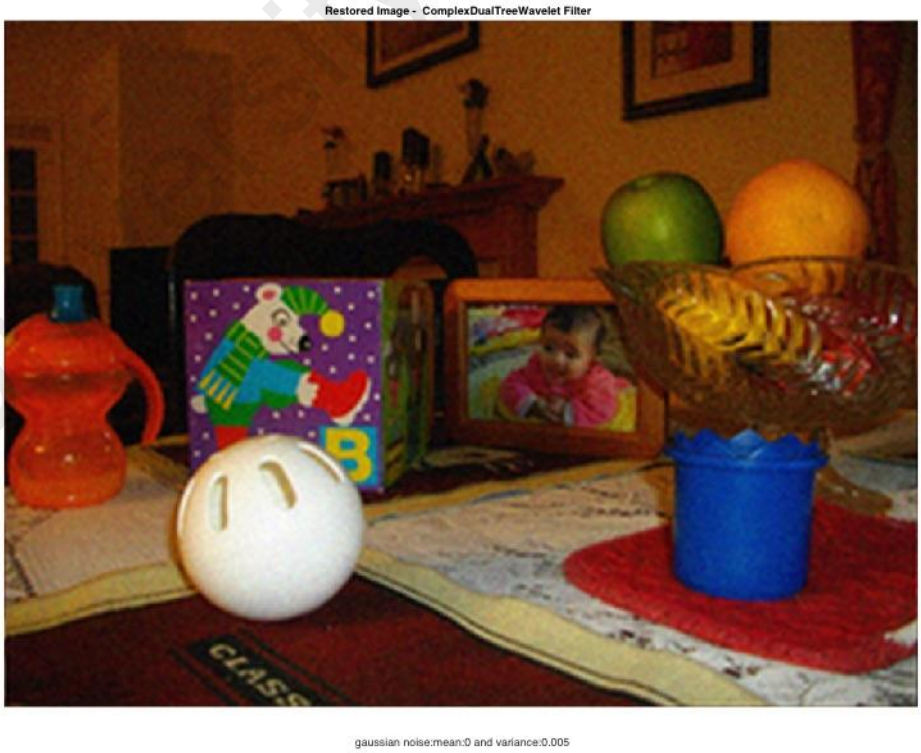

Figure 4.39 Restored Image using Complex Dual Tree Wavelet Filter in the present of Gaussian noise with 0 mean and 0.005 variance.

Figure 4.40 Restored Image using Complex Dual Tree Wavelet Filter in the present of Gaussian noise with 0 mean and 0.01 variance.

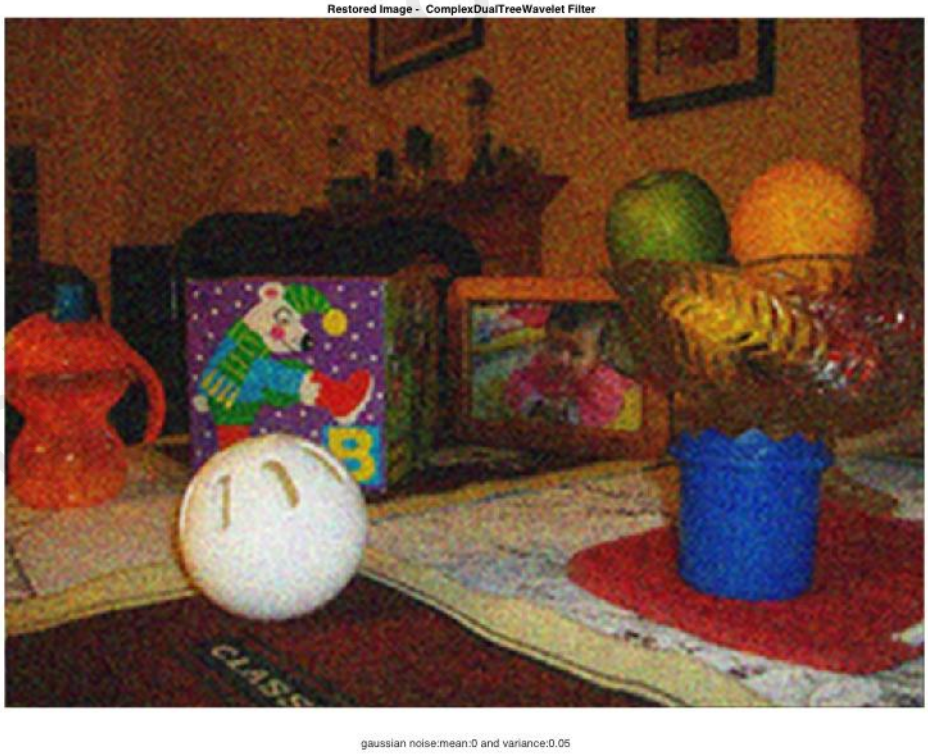

Figure 4.41 Restored Image using Complex Dual Tree Wavelet Filter in the present of Gaussian noise with 0 mean and 0.05 variance.

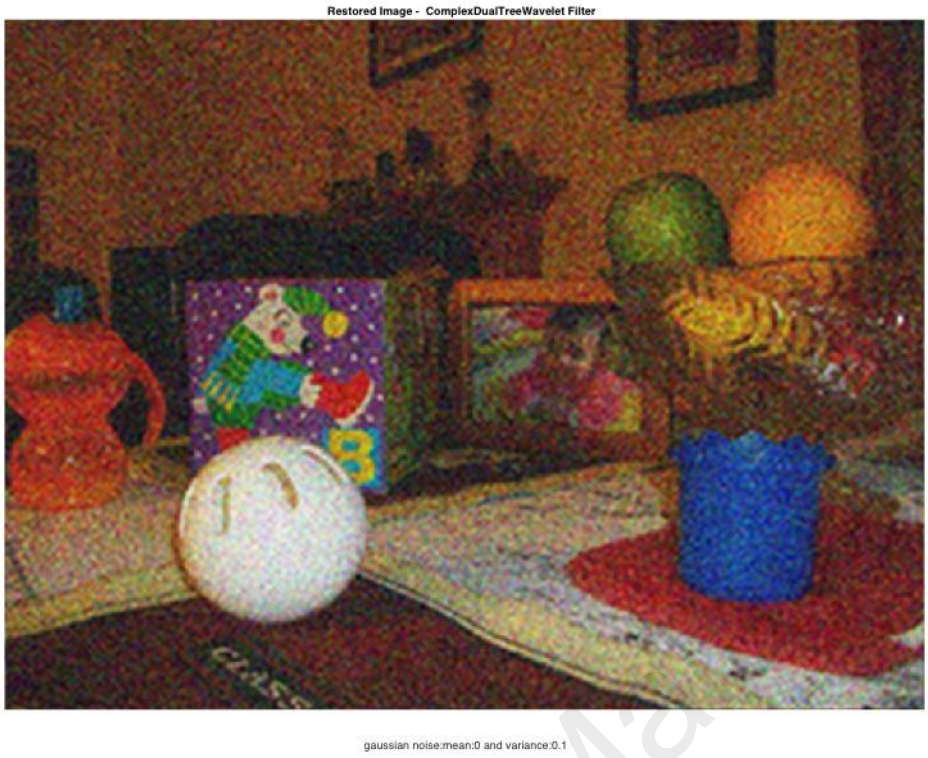

Figure 4.42 Restored Image using Complex Dual Tree Wavelet Filter in the present of Gaussian noise with 0 mean and 0.1 variance.

Figure 4.43 Restored Image using Complex Dual Tree Wavelet Filter in the present of Gaussian noise with 0 mean and 0.5 variance.

Figure 4.44 Restored Image using Complex Dual Tree Filter in the present of Salt &Pepper noise at 0.001 density.

Figure 4.45 Restored Image using Complex Dual Tree Filter in the present of Salt &Pepper noise at 0.005 density.

Figure 4.46 Restored Image using Complex Dual Tree Filter in the present of Salt &Pepper noise at 0.01 density.

Figure 4.47 Restored Image using Complex Dual Tree Filter in the present of Salt &Pepper noise at 0.05 density.

Figure 4.48 Restored Image using Complex Dual Tree Filter in the present of Salt &Pepper noise at 0.1 density.

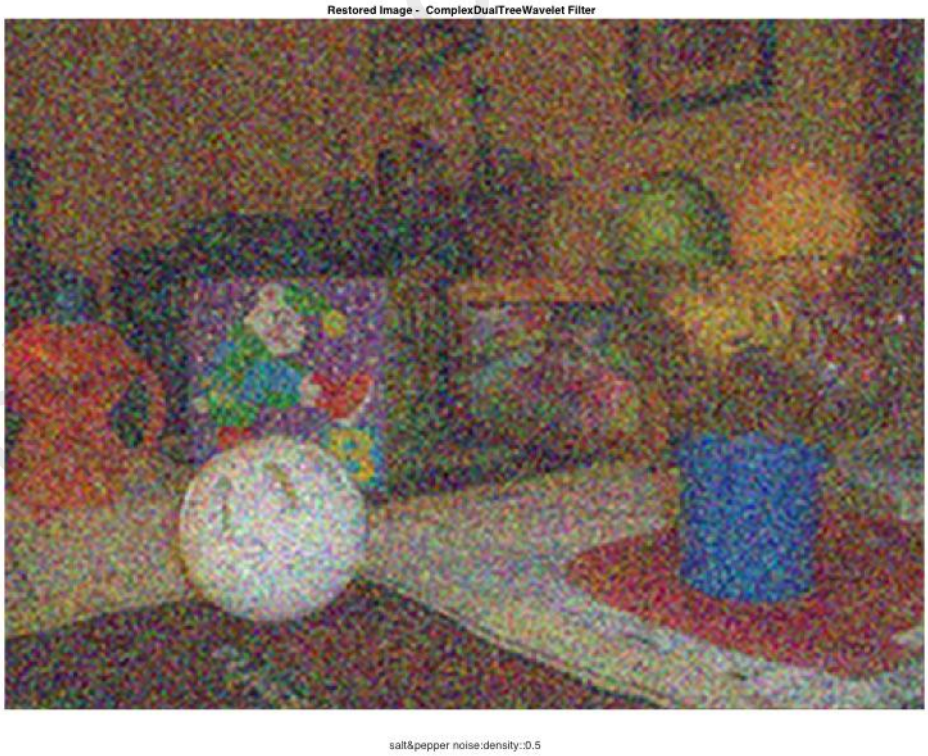

Figure 4.49 Restored Image using Complex Dual Tree Filter in the present of Salt &Pepper noise at 0.5 density.

Table 4.3 MSE, PSNR, and SSIM of Complex Dual Tree

Complex Wavelet Filter												
Quantitative Parameters	Gaussian Noise (Variance)						Salt & pepper Noise (Density)					
	0.001	0.005	0.01	0.05	0.1	0.5	0.001	0.005	0.01	0.05	0.1	0.5
MSE	0.0008	0.0011	0.0015	0.0050	0.0097	0.0389	0.0007	0.0008	0.0009	0.0019	0.0037	0.0388
PSNR (dB)	79.1223	77.7389	76.3915	71.1612	68.2522	62.2360	79.3952	78.9642	78.4541	75.2503	72.3988	62.2410
SSIM	0.9571	0.9313	0.9069	0.7906	0.7027	0.4266	0.9630	0.9558	0.9471	0.8868	0.8248	0.4330

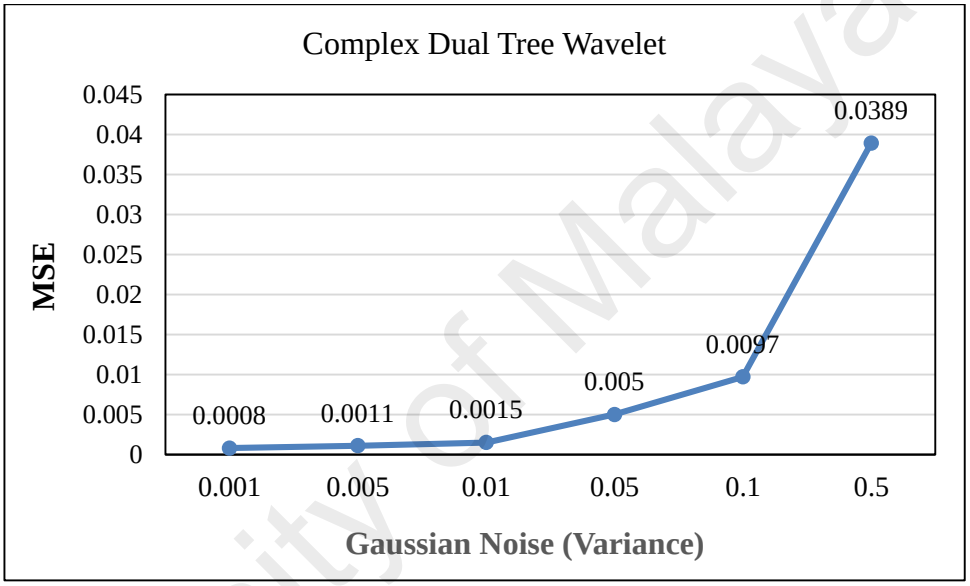

Figure 4.50 MSE of Complex Dual Tree Wavelet Inverse Filter for Gaussian Noise.

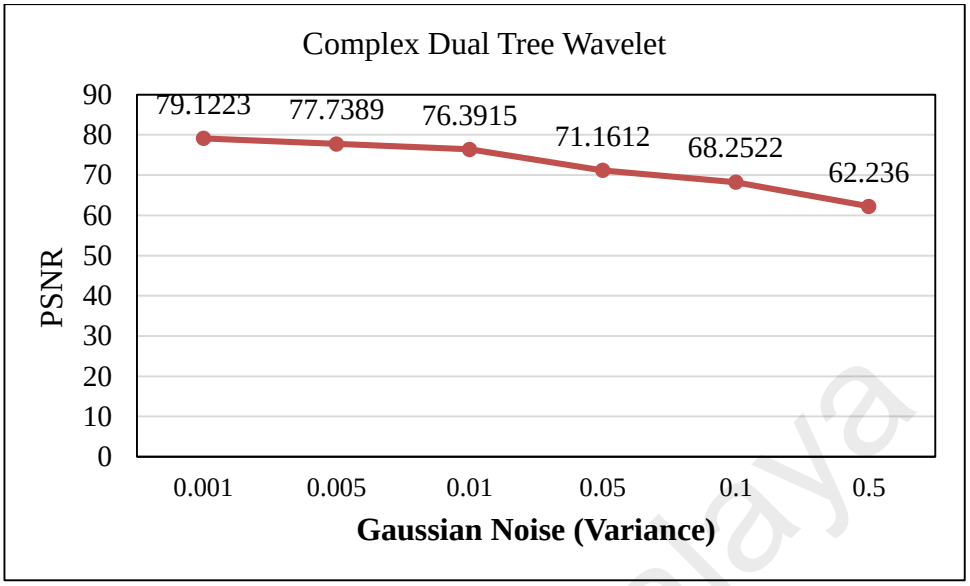

Figure 4.51 PSNR of Complex Dual Tree Wavelet Inverse Filter for Gaussian Noise.

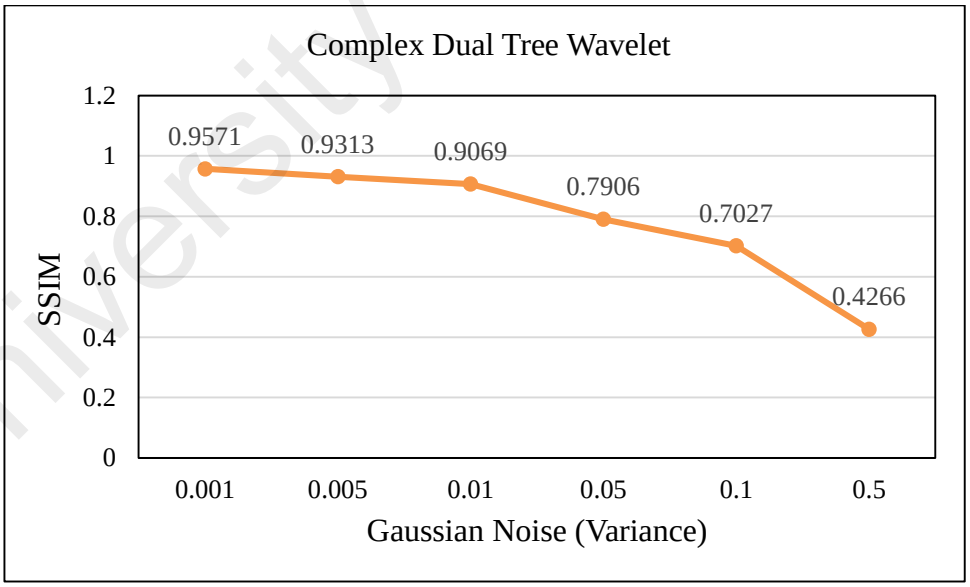

Figure 4.52 SSIM of Complex Dual Tree Wavelet Inverse Filter for Gaussian Noise

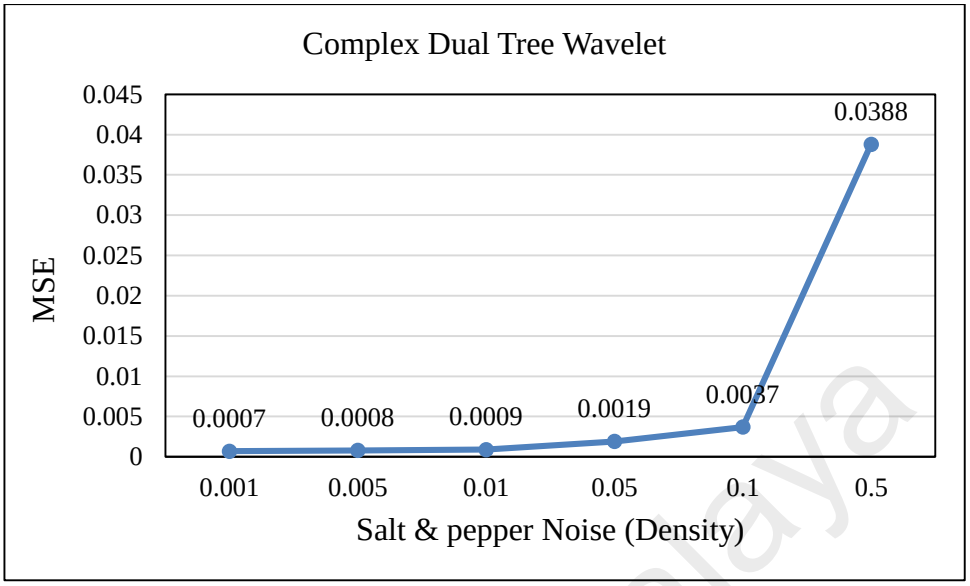

Figure 4.53 MSE of Complex Dual Tree Wavelet Inverse Filter for Salt & Pepper Noise

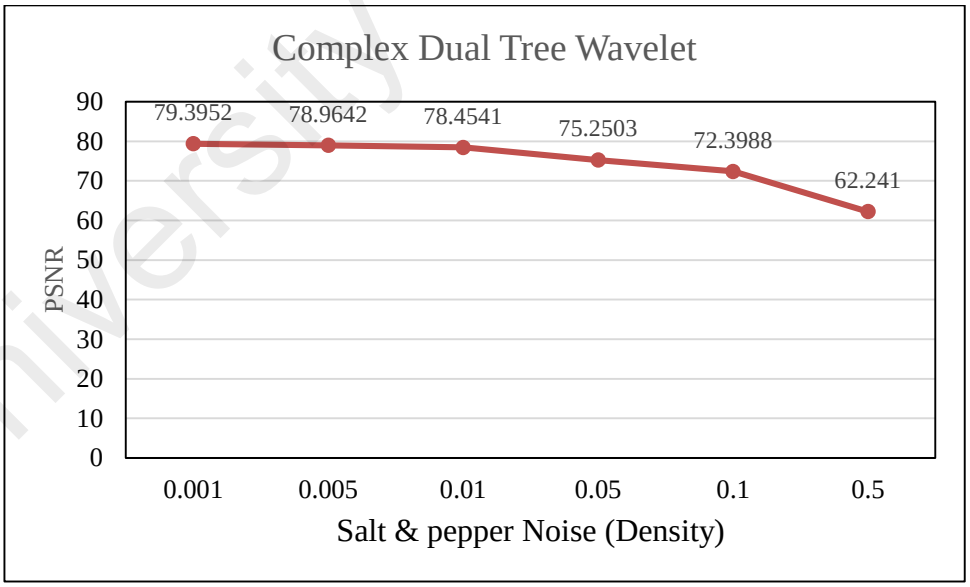

Figure 4.54 PSNR of Complex Dual Tree Wavelet Inverse Filter for Gaussian Noise

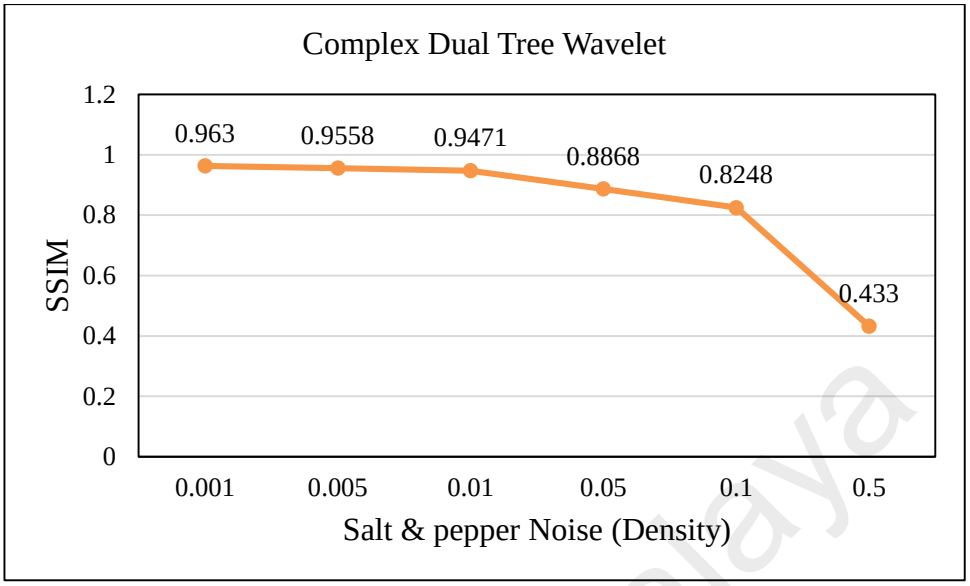

Figure 4.55 SSIM of Complex Dual Tree Wavelet Inverse Filter for Gaussian Noise

Complex Wavelet filter was exhibited the best an achievement compared with other methods that the restored images are similarly look like the original image. Quantitatively, The MSE, PSNR, and SSIM methods are calculated and presented as shown in Table 5.3. They were implemented to analyze and compare the result quality between the restored images and the original image. as compared to other methods, the cumulative squared errors in Wavelet filter were showed an extremely minimal value between the restored images and original images. Therefore, the qualities of the restored images were better. Thus, Table 5.3 showed that the noise increases, the cumulative error increases, and the quality of the restored image decreases. In addition, adding the noise to the original image, the results of the two noise methods showed that the salt and paper method was giving the better image quality compared with Gaussian Noise.

4.4 Comparison between Direct Inverse Filter, Wiener Filter and Wavelet Transform Filter

Table 5.4, 5.5, and 5.6 the MSE, PSNR, and SSIM of Direct Inverse, Wiener, and Complex Wavelet filters were compared based on the quality of the image. Direct Inverse filter is achieved the low quality of the image restoration technique due to its vulnerable with any type of noise. In contrast, Wiener filter showed a better quality than Direct Inverse filter but loses out to Complex Wavelet filters. Integration of the statistical properties of noise and original image into formulation of Wiener filter makes it more appropriate than Direct Inverse filter. Hence, the assumption in Wiener filter method that the statistical properties of noise and original image are well-known makes it badly unfeasible in practical. Consequently, the problem is to carefully evaluate the statistical properties of the original image till a satisfactory restored image is acquired. On the other hand, Complex Dual Tree Wavelet filter performed a high quality of image compared with other method such as Direct Inverse Filter and Wiener filter in all aspects of image quality assessment.

Table 4.4 MSE of Direct Inverse Filter, Wiener Filter, and Complex Dual Tree Wavelet.

Mean Square Error (MSE)												
Image Restoration Techniques	Gaussian Noise (Variance)						Salt & pepper Noise (Density)					
	0.001	0.005	0.01	0.05	0.1	0.5	0.001	0.005	0.01	0.05	0.1	0.5
Inverse	0.0034	0.0144	0.0273	0.1140	0.1987	0.4938	0.0015	0.0061	0.0121	0.0578	0.1149	0.5212
Wiener	0.0003	0.0008	0.0015	0.0064	0.0119	0.0399	0.0005	0.0016	0.0027	0.0063	0.0088	0.0411
Wavelet	0.0008	0.0011	0.0015	0.0050	0.0097	0.0389	0.0007	0.0008	0.0009	0.0019	0.0037	0.0388

Table 4.5 PSNR of Direct Inverse Filter, Wiener Filter, and Complex Dual Tree Wavelet.

Peak Signal Noise Ratio (PSNR)												
Image Restoration Techniques	Gaussian Noise (Variance)						Salt & pepper Noise (Density)					
	0.001	0.005	0.01	0.05	0.1	0.5	0.001	0.005	0.01	0.05	0.1	0.5
Inverse	72.8596	66.5363	36.7735	57.5599	55.1498	51.1951	76.4053	70.2806	67.3145	60.5118	57.5288	50.9605
Wiener	82.8322	78.9040	76.4449	70.0626	67.3851	62.1160	80.9869	76.0517	73.7709	70.1169	68.7009	61.9916
Wavelet	79.1223	77.7389	76.3915	71.1612	68.2522	62.2360	79.3952	78.9642	78.4541	75.2503	72.3988	62.2410

Table 4.6 SSIM of Direct Inverse Filter, Wiener Filter, and Complex Dual Tree Wavelet.

Structural Similarity Index (SSIM)												
Image Restoration Techniques	Gaussian Noise (Variance)						Salt & pepper Noise (Density)					
	0.001	0.005	0.01	0.05	0.1	0.5	0.001	0.005	0.01	0.05	0.1	0.5
Inverse	0.6492	0.3465	0.2368	0.0803	0.0484	0.0178	0.8902	0.7595	0.6274	0.2300	0.1186	0.0200
Wiener	0.9738	0.9396	0.9057	0.7542	0.6537	0.4067	0.9718	0.9273	0.8851	0.7720	0.7223	0.4130
Wavelet	0.9571	0.9313	0.9069	0.7906	0.7027	0.4266	0.9630	0.9558	0.9471	0.8868	0.8248	0.4330

CHAPTER 5: CONCLUSION AND FUTURE DEVELOPMENT

5.1 Conclusion

In this study, three image restoration techniques such as Direct Inverse Filter, Wiener filter, and Complex Wavelet filter were applied. These techniques were studied, derived, and implemented in MATLAB to reconstruct an original image that has intensively de-noising contaminated with either Gaussian noise or Salt and Pepper noise method at a variety of variances or densities. Then, image quality metrics, namely; mean square error (MSE), peak signal-to-noise ratio (PSNR), and structural similarity index (SSIM) are operated for evaluating and measuring the quality of the restored images. Consequently, the simulations and image quality metrics illustrated that Direct Inverse filter is poorest in restoring image because noise amplify at the nulls, so the noise becomes very large. Wiener filter outperforms Direct Inverse filter but the assumption that statistical properties of noise and original image are known makes it an impractical in practice. In addition, the wiener filter is the optimal filter for low amount of noise and cannot be used for large amount of noise because it assumes your process dynamics are linear, only provide a point estimate and can only handle processes with additive, unimodal noise. On the other hand, Complex Wavelet filter algorithm outperforms Wiener filter and Direct Inverse filter respectively, thus the Wavelet filter is the optimal filter for large amount of noise because have irregular shape which able to perfectly reconstruct functions with linear and higher order polynomial shapes such as rectangular and triangular. Principle of removing noise by applying a wavelet transform is that the noise typically associates to the high frequency information. Thus, noise information is frequently concentrated in sub blocks with infra-low frequency, infra-high frequency, and high frequency. Sub blocks with high frequency are practically constituted of noise information. Hence, if we fixed high frequency sub block to zero and suppress low frequency and high frequency sub blocks on certain inhibition, it can

obtain a certain effect of the noise removal. The performance of wavelet de-noising revealed that wavelet transform is fit to eliminate the image with a high frequency signal, In general. Complex Wavelet filter was showed the high quality of image compared with the following algorithms, Wiener filter, and Direct Inverse filter, respectively.

5.2 Future Development

In this research, applying different techniques of an image processing such as Direct Inverse Filter, Wiener Filter, and Wavelet Filter. For further studies, it is interesting to develop the techniques that used in this study and design a new technique of image restoration to improve the restoration of the noisy image.

REFERENCES

Beferull-Lozano, B., Xie, H., & Ortega, A. (2003). *Rotation-invariant features based on steerable transforms with an application to distributed image classification.* Paper presented at the Image Processing, 2003. ICIP 2003. Proceedings. 2003 International Conference on.

Bovik, A. C. (2010). *Handbook of image and video processing*: Academic press.

Chan, W. L., Choi, H., & Baraniuk, R. G. (2008). Coherent multiscale image processing using dual-tree quaternion wavelets. *IEEE Transactions on Image Processing, 17*(7), 1069-1082.

Chaux, C., Duval, L., & Pesquet, J.-C. (2006). Image analysis using a dual-tree M-band wavelet transform. *IEEE Transactions on Image Processing, 15*(8), 2397-2412.

Cohen, A., Daubechies, I., & Feauveau, J. C. (1992). Biorthogonal bases of compactly supported wavelets. *Communications on pure and applied mathematics, 45*(5), 485-560.

Daubechies, I. (1988). Orthonormal bases of compactly supported wavelets. *Communications on pure and applied mathematics, 41*(7), 909-996.

Eskicioglu, A. M., & Fisher, P. S. (1995). Image quality measures and their performance. *IEEE Transactions on communications, 43*(12), 2959-2965.

Garg, R., & Kumar, E. A. (2012). Comparison of various noise removals using Bayesian framework. *International Journal of Modern Engineering Research, 2*(1), 265-270.

Jalobeanu, A., Blanc-Féraud, L., & Zerubia, J. (2003). Satellite image deblurring using complex wavelet packets. *International Journal of Computer Vision, 51*(3), 205-217.

Kaur, S. (2015a). Noise types and various removal techniques. *International Journal of Advanced Research in Electronics and Communication Engineering (IJARECE) Volume, 4*.

Kaur, S. (2015b). Noise types and various removal techniques. *International Journal of Advanced Research in Electronics and Communication Engineering (IJARECE), 4*(2), 226-230.

Kovacvic, J., & Sweldens, W. (2000). Wavelet families of increasing order in arbitrary dimension. *IEEE Transactions on Image Processing, 9*(3), 280-496.

Li, W., Meunier, J., & Soucy, J.-P. (2006). *A 3D Adaptive Wiener Filter for Restoration of SPECT Images Using MRI as Reference Images.* Paper presented at the Engineering in Medicine and Biology Society, 2005. IEEE-EMBS 2005. 27th Annual International Conference of the.

Mallat, S. G. (1989). A theory for multiresolution signal decomposition: the wavelet representation. *IEEE transactions on pattern analysis and machine intelligence, 11*(7), 674-693.

Pillai, S., & Khadagade, S. (2017). A Review on Digital Image Restoration Process. *International Journal of Computer Applications, 158*(7).

Rani, V. (2013). A brief study of various noise model and filtering techniques. *Journal of global research in computer science, 4*(4), 166-171.

Selesnick, I. W., Baraniuk, R. G., & Kingsbury, N. C. (2005). The dual-tree complex wavelet transform. *IEEE signal processing magazine, 22*(6), 123-151.

Selesnick, I. W., & Li, K. Y. (2003). Video denoising using 2D and 3D dual-tree complex wavelet transforms. *Wavelets: Applications in Signal and Image Processing X, 5207*(2), 607-618.

Simoncelli, E. P., & Farid, H. (1996). Steerable wedge filters for local orientation analysis. *IEEE Transactions on Image Processing, 5*(9), 1377-1382.

Starck, J.-L., Candès, E. J., & Donoho, D. L. (2002). The curvelet transform for image denoising. *IEEE Transactions on Image Processing, 11*(6), 670-684.

Steffen, P., Heller, P. N., Gopinath, R. A., & Burrus, C. S. (1993). Theory of regular M-band wavelet bases. *IEEE Transactions on Signal Processing, 41*(12), 3497-3511.

Swaminathan, R. (2016). Application of Spatial Domain Filters on Noisy Images using MATLAB. *International Journal of Computer Applications, 134*(2), 27-30.

Sweldens, W. (1996). The lifting scheme: A custom-design construction of biorthogonal wavelets. *Applied and computational harmonic analysis, 3*(2), 186-200.

Xiong, C., Tian, J., & Liu, J. (2007). Efficient architectures for two-dimensional discrete wavelet transform using lifting scheme. *IEEE Transactions on Image Processing, 16*(3), 607-614.

Zhe, Z., & Wu, H. R. (2004). *A new way of pooling: starting from an image quality measure.* Paper presented at the Signal Processing, 2004. Proceedings. ICSP'04. 2004 7th International Conference on.